Palaeontology
The Palaeontological Association
www.palass.org

[Palaeontology, Vol. 62, Part 3, 2019, pp. 375–415]

THE EARLY COMPOSITION AND EVOLUTION OF THE TURTLE SHELL (REPTILIA, TESTUDINATA)

by TOMASZ SZCZYGIELSKI[1,2] *and* TOMASZ SULEJ[1]

[1]Institute of Paleobiology, Polish Academy of Sciences, Twarda 51/55, Warsaw, 00-818, Poland; t.szczygielski@twarda.pan.pl
[2]Department of Paleobiology & Evolution, Faculty of Biology, Biological & Chemical Research Centre, University of Warsaw, Żwirki i Wigury 101, Warsaw, 02-089, Poland

Typescript received 20 July 2018; accepted in revised form 13 September 2018

Abstract: The shell of the oldest true turtle (Testudinata) branch (Proterochersidae) from the Late Triassic (Norian) of Poland and Germany was built in its anterior and posterior part from an osteodermal mosaic which developed several million years after the plastron, neurals and costal bones. We provide the most detailed description of the shell composition in proterochersids to date, together with a review of the shell composition in other Triassic pantestudinates. A scenario of early evolution of the turtle shell is proposed based on new data, and the possible adaptive meaning of the observed evolutionary changes is discussed. These observations are consistent with the trend of shell simplification previously reported in turtles. Several aspects of proterochersid shell anatomy are intermediate between *Odontochelys semitestacea* and more derived turtles, supporting their stem phylogenetic position. Three additional ossifications were sutured to xiphiplastra and pelvis in *Proterochersis* spp. and at least in some individuals the nuchal bone was paired. The peripherals, suprapygals, and pygal bone are most likely to be of osteodermal origin and homologous to the proterochersid shell mosaic.

Key words: Testudinata, dermal armour, Proterochersidae, Norian, carapace evolution, turtle shell.

THE shell of turtles is a unique structure, originating from modifications of co-opted morphogenetic pathways, which lead to coordinated changes in the development of the pectoral girdle, axial skeleton, musculature and integumentary skeleton, resulting in profound alterations of the general body plan and function of these animals (Burke 1989, 1991; Gilbert *et al.* 2001, 2008; Loredo *et al.* 2001; Cebra-Thomas *et al.* 2005; Nagashima *et al.* 2007, 2009, 2012, 2013*a*; Kuratani *et al.* 2011; Rice *et al.* 2015, 2016). It usually consists of 50 bones building the carapace and 9 bones forming the plastron (Zangerl 1969), but more elements were present in the earliest turtles (Fraas 1913; Gaffney 1985, 1990; Szczygielski & Sulej 2016; Joyce 2017; Szczygielski 2017). Despite intensive research since the beginning of the nineteenth century, the exact nature and homologies of many of the shell elements remain enigmatic and controversial (see Szczygielski & Sulej (2018*a*, tables S1, S2) for lists of opinions on the homology of shell-building elements and an extended discussion) and until the end of the first decade of the twenty-first century nothing was known about their early evolution.

The fossil record of shell formation is patchy. Until recently, the oldest reasonably complete turtles were *Proterochersis robusta* Fraas, 1913 and *Proganochelys quenstedti* Baur, 1887*a* from the Norian of Germany, and *Palaeochersis talampayensis* Rougier *et al.*, 1995 from the Norian–Rhaetian of Argentina. A roughly contemporary, but very incomplete taxon was found in Thailand (de Broin *et al.* 1982) and later named *Proganochelys ruchae* de Broin, 1984, and a more complete turtle was reported as cf. *Proganochelys*, but not described in detail, from Greenland (Jenkins *et al.* 1994). Several other very fragmentary historical turtle finds were described from the Triassic, but most of them turned out to be misinterpreted remains of other animals (see Joyce (2017) for a comprehensive review). Each of the above mentioned taxa already possessed a well-developed carapace and plastron. Additionally, the shells of the Triassic taxa are usually ankylosed, obliterating the sutures and making it very difficult or impossible to assess the number, position and shape of shell-building elements (Gaffney 1985, 1990; Sterli *et al.* 2007; Szczygielski & Sulej 2016). For that reason, the shell composition in these taxa was parsimoniously assumed to be the same as that of more derived turtles, with only an additional pair of costal bones or mesoplastra accepted in some of them, and supernumerary peripherals inferred based on marginal scute number (Fraas 1913; Gaffney 1985, 1990). In particular, the nuchal and pygal regions of the shell remain enigmatic,

doi: 10.1111/pala.12403

there being absolutely no data about their bone composition and suture layout in any of the Triassic testudinates (Fraas 1913; Gaffney 1985, 1990; Rougier *et al.* 1995; Sterli *et al.* 2007; Szczygielski & Sulej 2016; Joyce 2017).

Classically, it has been assumed that the turtle ancestor had its body covered with numerous osteoderms, which subsequently fused to the vertebrae and ribs, giving rise to costals and neurals (Owen 1849; Baur 1887*a*; Hay 1898, 1922, 1929; Gadow 1909; Versluys 1914*a*, *b*; Deraniyagala 1930; Kälin 1945; Gregory 1946; Lee 1993, 1996, 1997; Scheyer *et al.* 2008) or were pushed aside and replaced by the costals and neurals, after their initial development below the dermis (Hay 1929; Deraniyagala 1930). The former hypothesis was seemingly supported by the discovery of *Chinlechelys tenertesta* Joyce *et al.*, 2009 (*Proganochelys tenertesta* of Joyce 2017), a Norian turtle with a paper-thin carapace, apparently only weakly attached to the ribs, and osteoderms composed of numerous ossifications (Lucas *et al.* 2000; Joyce *et al.* 2009; Lichtig & Lucas 2015, 2016). This conception is, however, now considered obsolete thanks to recently discovered, older and earlier stem turtles, which are devoid of body osteoderms. The Ladinian *Pappochelys rosinae* Schoch & Sues, 2015 lacked any elements of the shell, but had broadened ribs and forked, broadened gastralia, reminiscent of early stages of plastron bone development (Schoch & Sues 2015, 2016, 2018). Slightly younger, Carnian *Odontochelys semitestacea* Li *et al.*, 2008 possessed a well-developed plastron, broadened (but still not sutured together) ribs and a row of probable neural bones along the back. All of the dermal ossifications of the carapace appeared in turtles more derived than *O. semitestacea*, after the costals, neurals and plastron developed, and all the Norian turtles already had complete shells (Fraas 1913; de Broin *et al.* 1982; de Broin 1984; Gaffney 1985, 1990; Jenkins *et al.* 1994; Rougier *et al.* 1995; Sterli *et al.* 2007; Joyce *et al.* 2009; Szczygielski & Sulej 2016; Joyce 2017).

The general sequence of appearance of the shell elements is thus known but, as a result of frequent shell ankylosis and incompleteness of the Triassic turtle remains, almost no data are available on the evolutionary origin and early composition of the fully dermal parts of the carapace; formed by the nuchal, peripheral, pygal and suprapygal bones. Fortunately, some new observations on the specimens of *Proterochersis robusta* (Figs 1–8, 16N; Szczygielski & Sulej 2018*a*, figs S1A–C, S3A, C, movies S1–S3) and the new material of *Proterochersis porebensis* Szczygielski & Sulej, 2016 (Figs 9–15, 16A–M, 17–19; Szczygielski & Sulej 2018*a*, figs S2, S4C–H, movies S4–S7, models S1–S2) provide additional data about the initial composition and layout of these dermal elements. Especially interesting is the presence of a mosaic of numerous osteoderms in the anterior and posterior sections of the carapace of *Proterochersis* spp., reported here for the first time. Such a morphology has never been observed in Mesozoic turtles with the exception of the very fragmentary *Chinlechelys tenertesta* from the USA (Lichtig & Lucas 2015, 2016). Given the position of proterochersids, represented by *Prot. robusta*, *Prot. porebensis* and *Keuperotesta limendorsa* Szczygielski & Sulej, 2016 (*Proterochersis limendorsa* of Joyce 2017) as the oldest true turtles (Testudinata), this allows for some meaningful insight into the processes occurring during the coalescence of the dorsal and ventral parts of the turtle shell into the complete structure.

Institutional abbreviations. CSMM, Carl-Schweizer-Museum, Murrhardt, Germany; IVPP, Institute of Vertebrate Paleontology and Paleoanthropology, Chinese Academy of Sciences, Beijing, China; NMMNH, New Mexico Museum of Natural History and Science, Albuquerque, USA; PULR, Universidad Nacional de La Rioja, La Rioja, Argentina; SMNS, Staatliches Museum für Naturkunde, Stuttgart, Germany; ZPAL; Roman Kozłowski Institute of Paleobiology, Polish Academy of Sciences, Warsaw, Poland.

MATERIAL

All of the existing specimens of *Proterochersis porebensis* (ZPAL V.39V.39/1–28, ZPAL V.39V.39/34, ZPAL V.39V.39/48–72, ZPAL V.39V.39/155–300, ZPAL V.39V.39/331–366, ZPAL V.39V.39/370, ZPAL V.39/373–404, ZPAL V.39/416–420, and uncatalogued) were studied. The material of *Proterochersis robusta*, *Keuperotesta limendorsa*, *Pappochelys rosinae*, *Odontochelys semitestacea*, *Proganochelys quenstedti*, *Palaeochersis talampayensis*, *Chinlechelys tenertesta* and *Priscochelys hegnabrunnensis* Karl, 2005, was studied first-hand in the corresponding collections. See Szczygielski & Sulej (2018*a*) for more detailed descriptions of the referred material.

Pappochelys rosinae *(Pantestudinata; Ladinian)*

Pappochelys rosinae comes from the Middle Triassic strata of the Erfurt Formation in Eschenau, Germany. Out of several studied specimens, three will be mentioned in this work as comparative material: SMNS 92360, SMNS 91606, SMNS 91895.

Odontochelys semitestacea *(Pantestudinata; Carnian)*

The specimens of *Odontochelys semitestacea* were described from Guanling, China (Li *et al.* 2008). The material studied by us consists of the paratype (IVPP V 13240) and IVPP V15653.

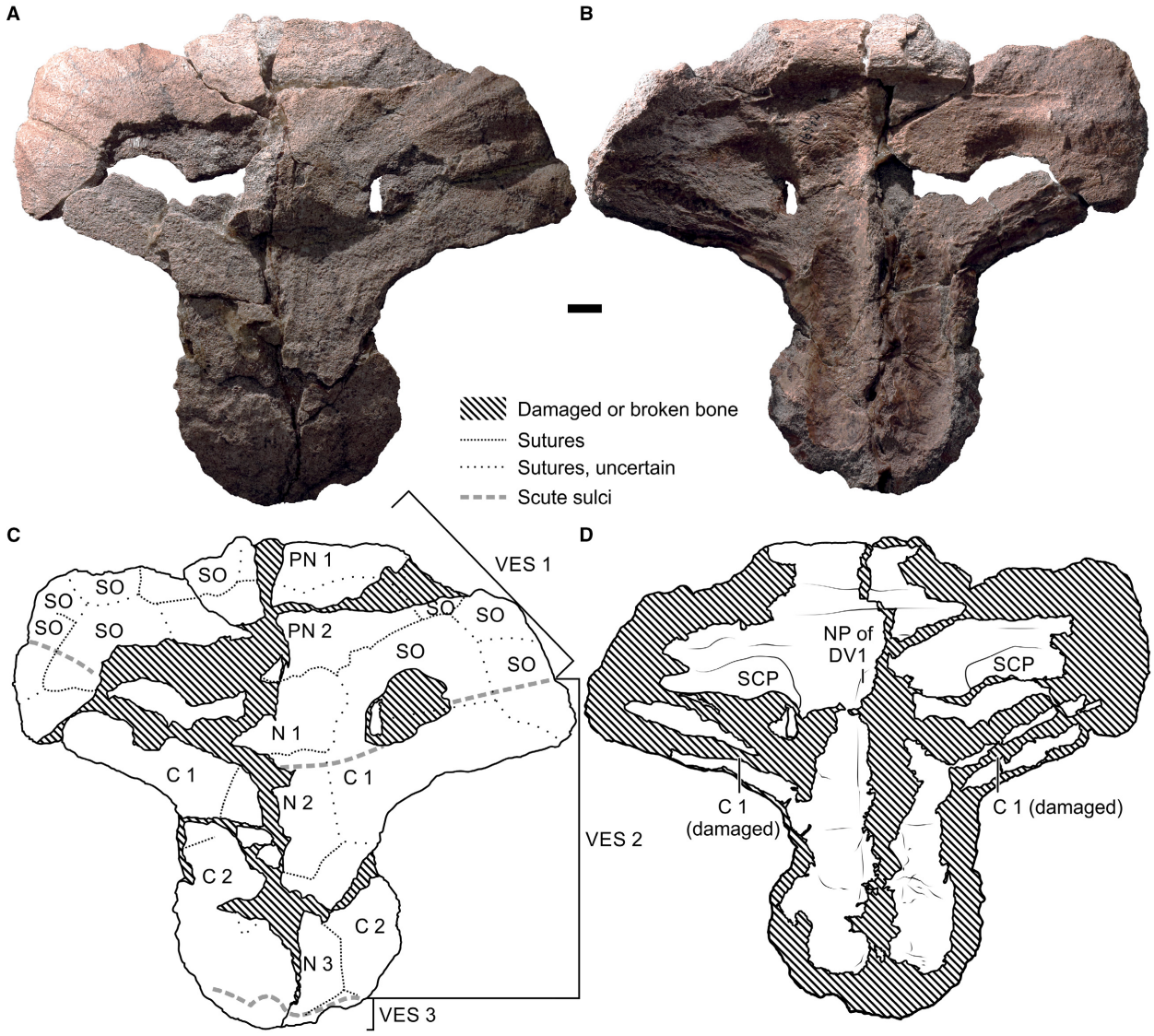

FIG. 1. *Proterochersis robusta*, SMNS 16442, anterior section of the carapace. A, C, dorsal view; B, D, visceral view. *Abbreviations*: C, costal bone; DV, dorsal vertebra; N, neural bone; NP, neural process; PN, preneural bone; SCP, scapular pit; SO, supernumerary ossification; VES, vertebral scute. Scale bar represents 1 cm. Colour online.

Proterochersis robusta *(Testudinata: Proterochersidae; Norian)*

All of the existing specimens historically attributed to *Proterochersis robusta*, *Prot.* '*intermedia*' and '*Murrhardtia staeschei*' (SMNS 11396, 12777, 15479, 16442, 16603, 16668, 17561, 17755, 17755a, 17756, 17930, 18440, 19103, 50917, 51441, 56606, 81917; CSMM uncat.) were studied with exception of SMNS 50918. The most important for this research are CSMM uncat., SMNS 11396, SMNS 12777, SMNS 16442, SMNS 16603, SMNS 17755, SMNS 17755a and SMNS 18440.

SMNS 17755 and SMNS 18440 lack any diagnostic regions that could differentiate them from *Keuperotesta limendorsa*, but they come from Murrhardt, where several specimens representing only *Proterochersis robusta* were found (CSMM uncat., SMNS 16442, SMNS 17561, SMNS 17755a). Therefore, we tentatively assign them to *Prot. robusta*, together with other un-diagnostic specimens from that locality: SMNS 17756 (partial natural mould of the inside of the carapace, consisting of imprints of four ribs and costovertebral tunnel, and some scraps of bone), SMNS 50917 (a fragmentary plastron, consisting of a poorly preserved bridge and a fragment of the area of the right pectoral scute, a nearly complete right first and second abdominal, a complete right femoral and anal, and fragments of the left femoral and anal scute areas, with attached bases of the ilia, left lateral

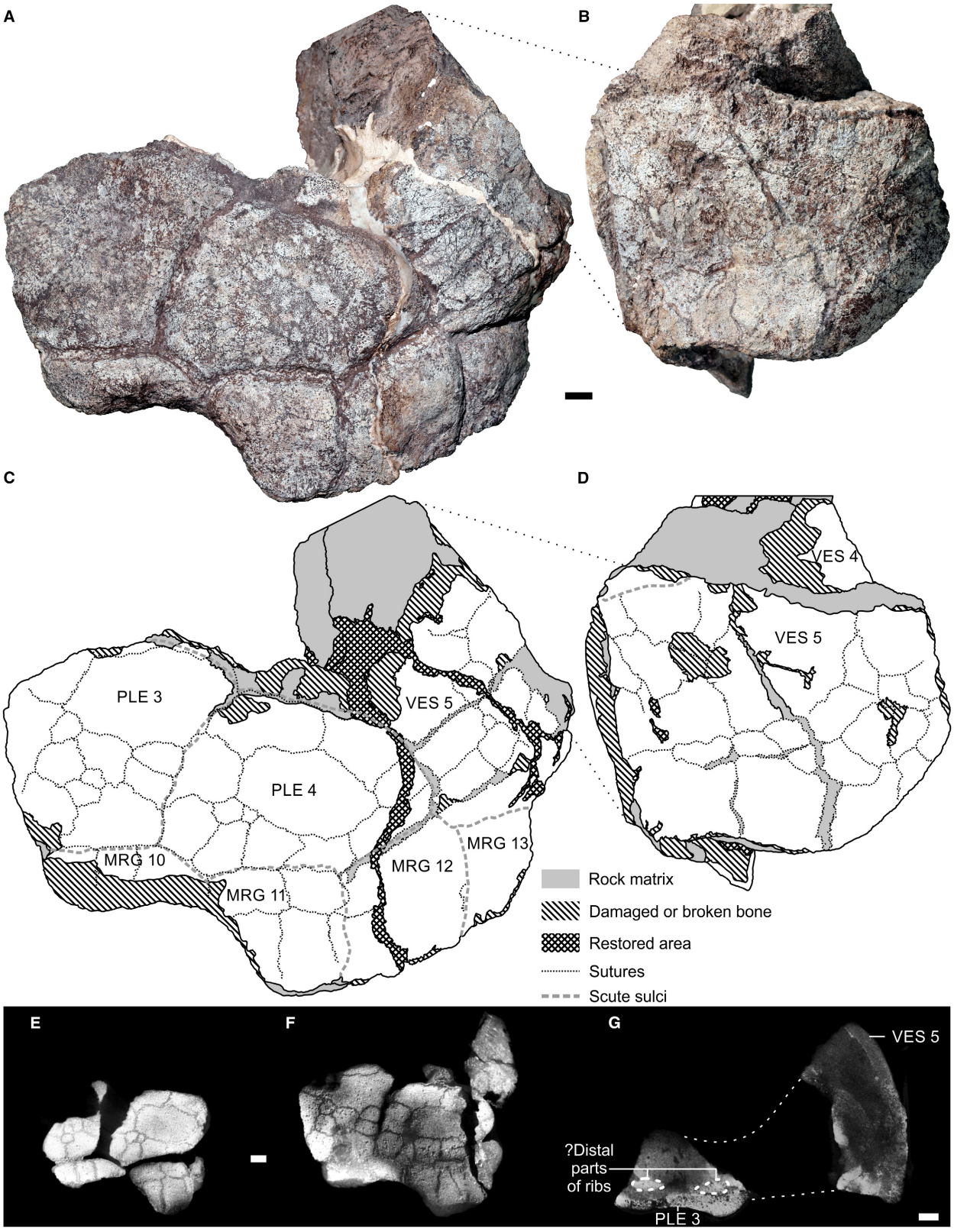

FIG. 2. *Proterochersis robusta*, SMNS 17755a, posterior left region of the carapace. A, C, lateral view. B, D, dorsoposterior view. E–G, CT scans in lateral (E, F) and dorsoventral (G) view. Note the distal sections of the ribs (G) separate from the mosaic. *Abbreviations*: MRG, marginal scute; PLE, pleural scute; VES, vertebral scute. Scale bars represent 1 cm. Colour online.

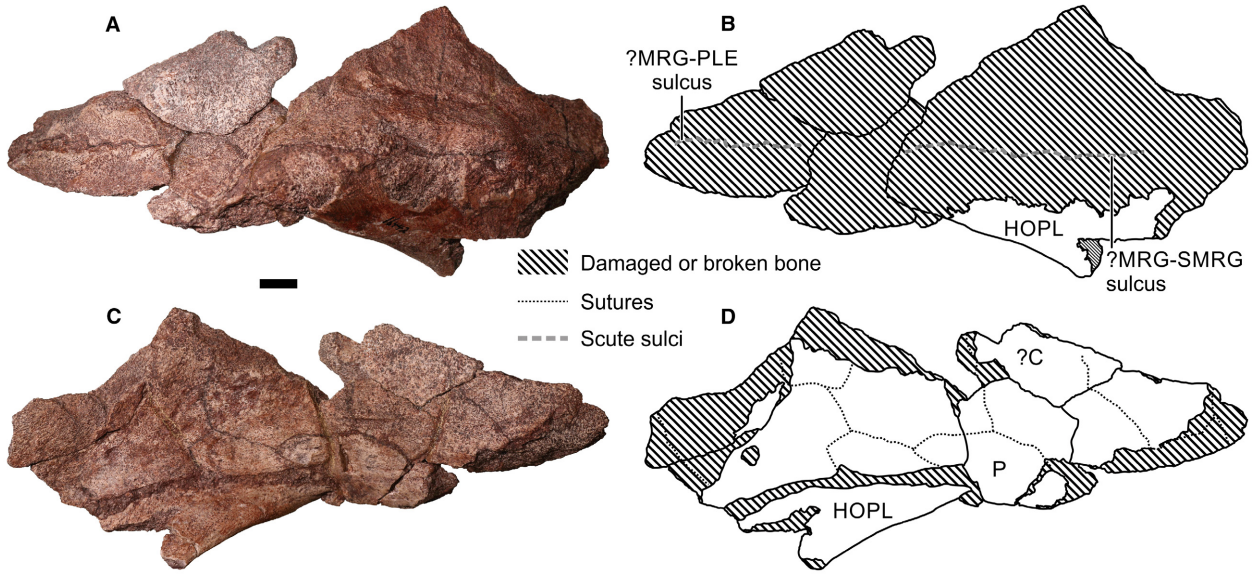

FIG. 3. *Proterochersis robusta*, SMNS 16442, left anterior marginal section of the shell. A–B, lateral view. C–D, visceral view. *Abbreviations*: C, costal bone; HOPL, hyoplastron; MRG, marginal scute; P, peripheral bone; PLE, pleural scute; SMRG, supramarginal scute. Scale bar represents 1 cm. Colour online.

pubic process and the epipubic process), SMNS 56606 (a pelvis of a young specimen with eroded posterior parts of the carapace and plastron and three posteriormost dorsal vertebrae with corresponding rib heads) and SMNS 81917 (an incomplete right hyoplastron of a young, not fully ossified specimen). Three other specimens, SMNS 15479 (a double imprint of the ventral surface of a plastron from Steinbruck, figured by Gaffney 1990), SMNS 16668 (a partial internal mould of the carapace, found in Welzheim) and SMNS 19103 (a partial internal mould of a carapace, found in Engelberg) lack diagnostic features that would allow an identification more precise than Proterochersidae indet. SMNS 17561 (a mostly complete shell from Murrhardt), SMNS 17930 (an internal mould of a carapace and most of the carapace itself, lacking the bridge section of the right rim, whole left rim, and a large part of the posterior left region, found in Oberbrüden) and SMNS 51441 (an internal mould of the shell, found in Strümpfelbach; SMNS houses a plastic mould of the original exhibited in Steinzeitmuseum in Kleinheppach) are identifiable as *Proterochersis robusta* but display no characters useful to this study.

Proterochersis porebensis *(Testudinata, Proterochersidae; Norian)*

The studied material of *Proterochersis porebensis* comes from the Late Triassic locality of Poręba, Poland. See Sulej *et al.* (2012), Niedźwiedzki *et al.* (2014), Zatoń *et al.* (2015) and Szczygielski & Sulej (2016) for information about the locality and its ecosystem in the Triassic. The specimens most important for this research are: ZPAL V.39V.39/3, ZPAL V.39V.39/4, ZPAL V.39V.39/5, ZPAL V.39V.39/8, ZPAL V.39/11, ZPAL V.39/13, ZPAL V.39/14, ZPAL V.39/20, ZPAL V.39/21, ZPAL V.39/22, ZPAL V.39/23, ZPAL V.39/48, ZPAL V.39/49, ZPAL V.39/51, ZPAL V.39/54, ZPAL V.39/55, ZPAL V.39/59, ZPAL V.39/68, ZPAL V.39/69, ZPAL V.39/167, ZPAL V.39/168, ZPAL V.39/170, ZPAL V.39/173, ZPAL V.39/181, ZPAL V.39/213, ZPAL V.39/235,ZPAL V.39/373, ZPAL V.39/374, ZPAL V.39/375, and ZPAL V.39/376, ZPAL V.39/404, ZPAL V.39/416, ZPAL V.39/417, ZPAL V.39/418, ZPAL V.39/419.

Keuperotesta limendorsa *(Testudinata, Proterochersidae; Norian)*

The holotype and only known specimen of *Keuperotesta limendorsa* (SMNS 17757) consists of a partial shell with scapulocoracoids, posterior cervical vertebrae and anterior caudal vertebrae. It was found near Rudersberg, Germany, and was described and figured by Joyce *et al.* (2013), Szczygielski & Sulej (2016) and Szczygielski (2017). Joyce (2017) expressed opinion that since this species was found by us (Szczygielski & Sulej 2016) to be the sister taxon of *Proterochersis porebensis* and *Prot. robusta*, it may also be nested within the genus *Proterochersis*. While this may be true and its generic distinctiveness is based on somewhat subjective merits (there is a

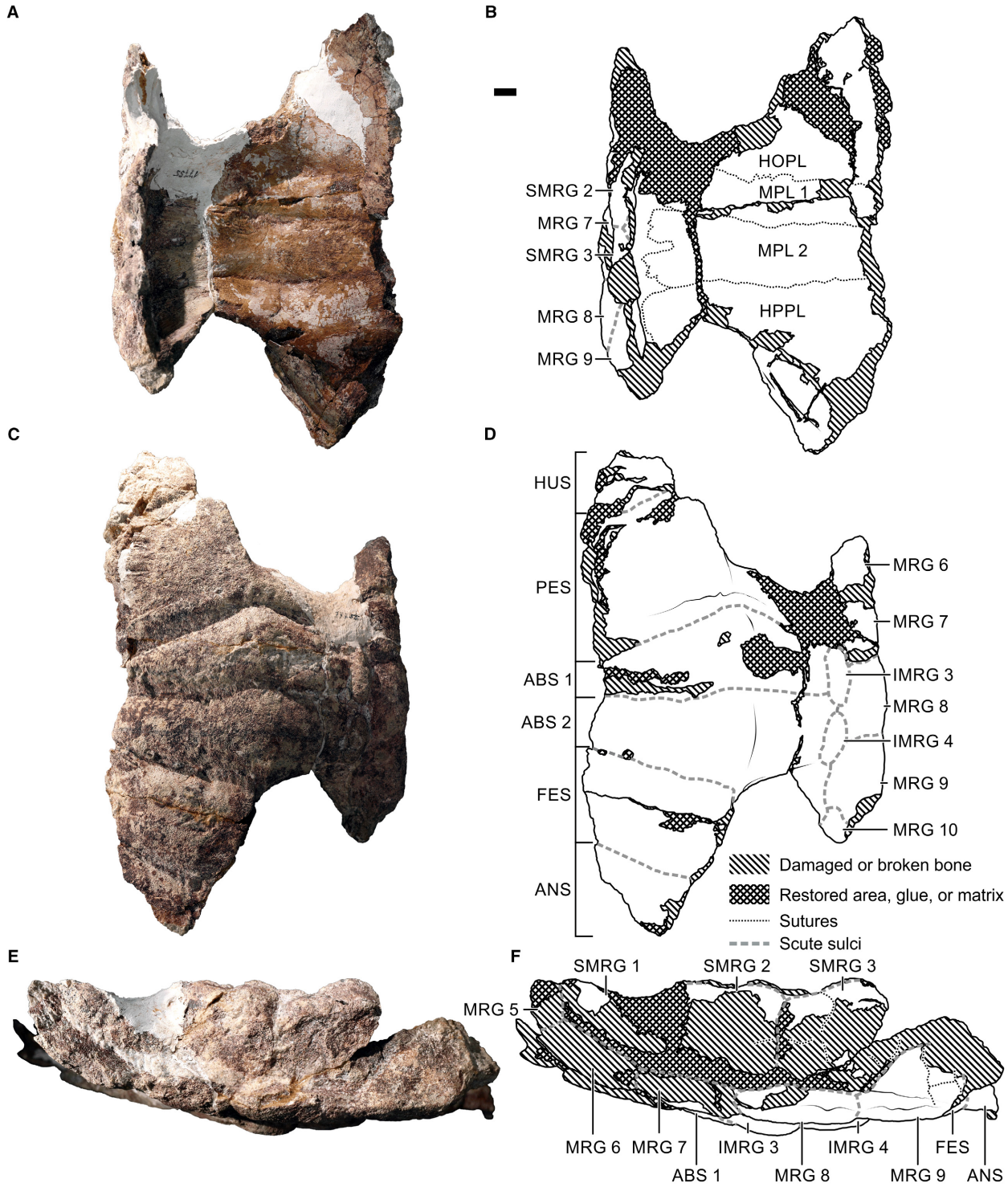

FIG. 4. *Proterochersis robusta*, SMNS 17755, left bridge and part of the plastron. A–B, dorsal view; C–D, ventral view; E–F, lateral view. *Abbreviations*: ABS, abdominal scute; ANS, anal scute; FES, femoral scute; HOPL, hyoplastron; HPPL, hypoplastron; HUS, humeral scute; IMRG, inframarginal scute; MPL, mesoplastron; MRG, marginal scute; PES, pectoral scute; SMRG, supramarginal scute. Scale bar represents 1 cm. Colour online.

notably larger difference between SMNS 17757 and all the other *Proterochersis* specimens than between *Prot. robusta* and *Prot. porebensis*; but on the other hand, the palaeotaxonomic opinions are frequently subjective) at this time too little is known about that taxon and the biodiversity of the Triassic turtles in

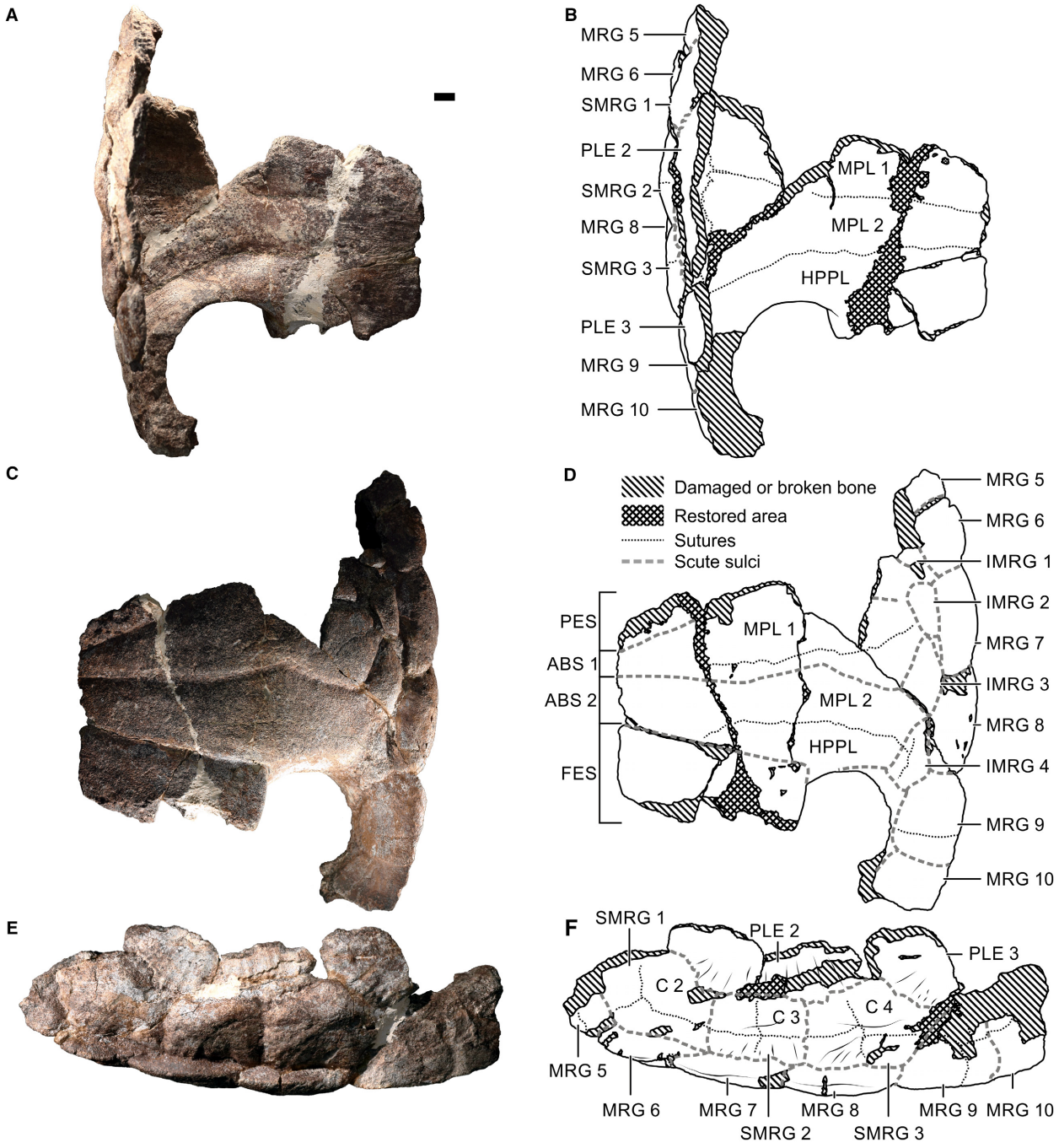

FIG. 5. *Proterochersis robusta*, SMNS 18440, left bridge and part of the plastron. A–B, dorsal view. C–D, ventral view. E–F, lateral view. *Abbreviations*: ABS, abdominal scute; C, costal bone; FES, femoral scute; HPPL, hypoplastron; IMRG, inframarginal scute; MPL, mesoplastron; MRG, marginal scute; PES, pectoral scute; PLE, pleural scute; SMRG, supramarginal scute. Scale bar represents 1 cm. Colour online.

general to substantially support or reject that view, and more data are needed. Until this taxon is better understood and included in more phylogenetic analyses, this remains a largely semantic question, and we prefer to use the name *Keuperotesta* to highlight the differences between that turtle and *Proterochersis* spp. *sensu* Szczygielski & Sulej (2016) and keep the naming consistent. This approach agrees with that proposed recently by Parker (2018) to keep the taxonomic stability of fossil taxa.

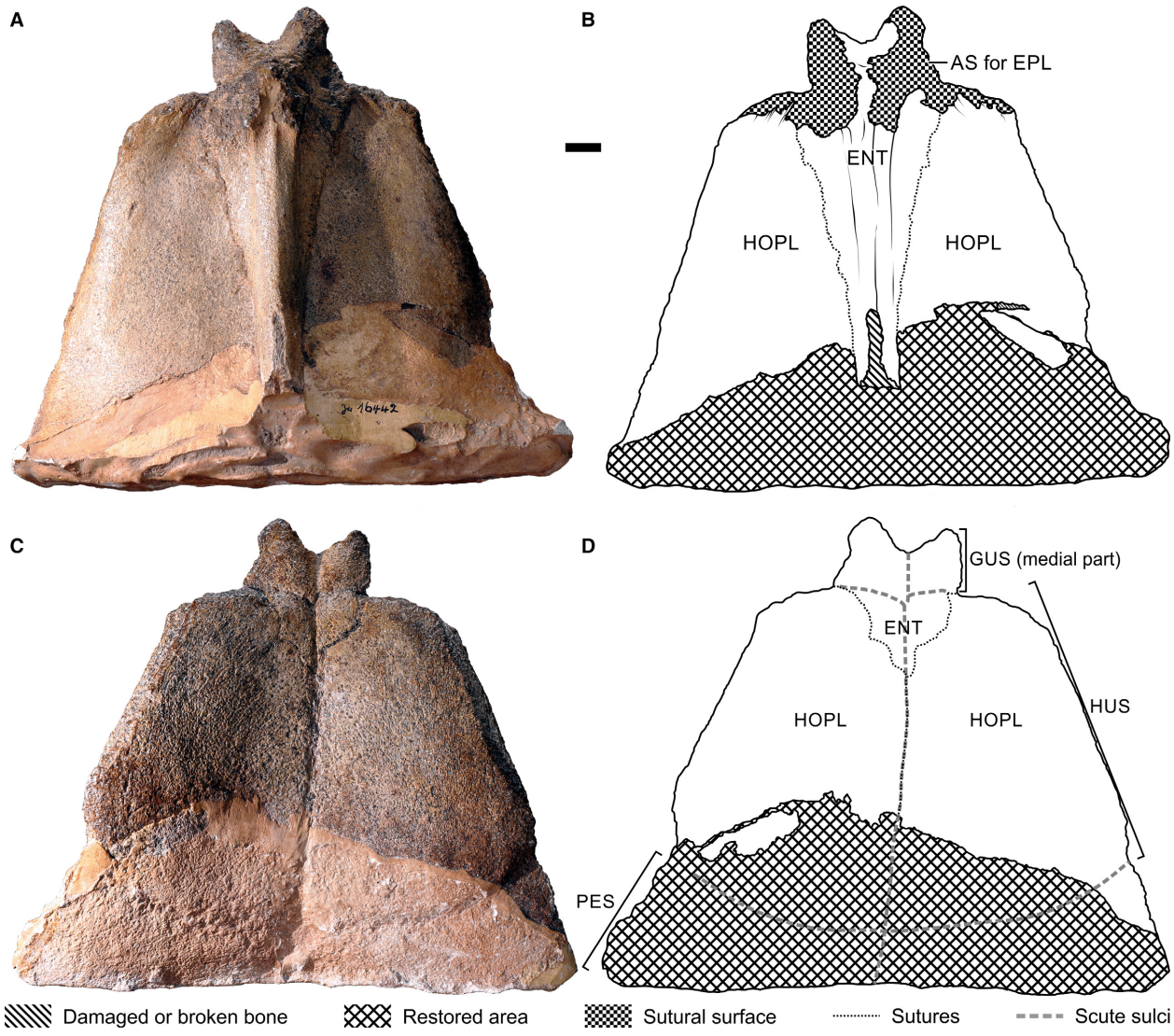

FIG 6. *Proterochersis robusta*, SMNS 16442. Anterior plastral lobe in visceral (A–B) and ventral (C–D) view. The restored section of the specimen is a plaster cast of the natural mould of ventral surface of that specimen. *Abbreviations*: AS, articulation site; ENT, entoplastron; EPL, epiplastron; GUS, gular scute; HOPL, hyoplastron; HUS, humeral scute; PES, pectoral scute. Scale bar represents 1 cm. Colour online.

Proganochelys quenstedti *(Testudinata, Proganochelyidae; Norian)*

Several specimens of *Proganochelys quenstedti* housed in Staatliches Museum für Naturkunde (Gaffney 1985 presented a preliminary description of part of the available material; see Gaffney 1990 for a list, figures and detailed descriptions of all of them) were studied by one of us (TSz). Out of them, three are the most important for this study, all coming from Trossingen, Germany: SMNS 16980, SMNS 17203 and SMNS 17204.

Joyce (2017) chose to use the specific epithet *quenstedtii* and considered the spelling *quenstedti* to be incorrect. While it is true that Baur (1887*b*) used the spelling *quenstedtii* and no explicitly intentional emendation that we know of has been published since, we think that name *quenstedti* should be considered correct; it arguably is subject to article 32.5 of ICZN (1999) (Baur clearly stated that he names the new species after Quenstedt, so the grammatically incorrect form *quenstedtii* may be treated as a *lapsus calami* or a printing error) and even if that is deemed irrelevant in this particular case, the name is arguably subject to articles 33.2.3.1 and/or 33.3.1 of ICZN (1999) (it is prevalent in modern literature and thus considered correct). Resurrection of the original but grammatically incorrect and now mostly forgotten spelling would probably only cause further confusion and lead to both versions of the same name functioning in parallel in the

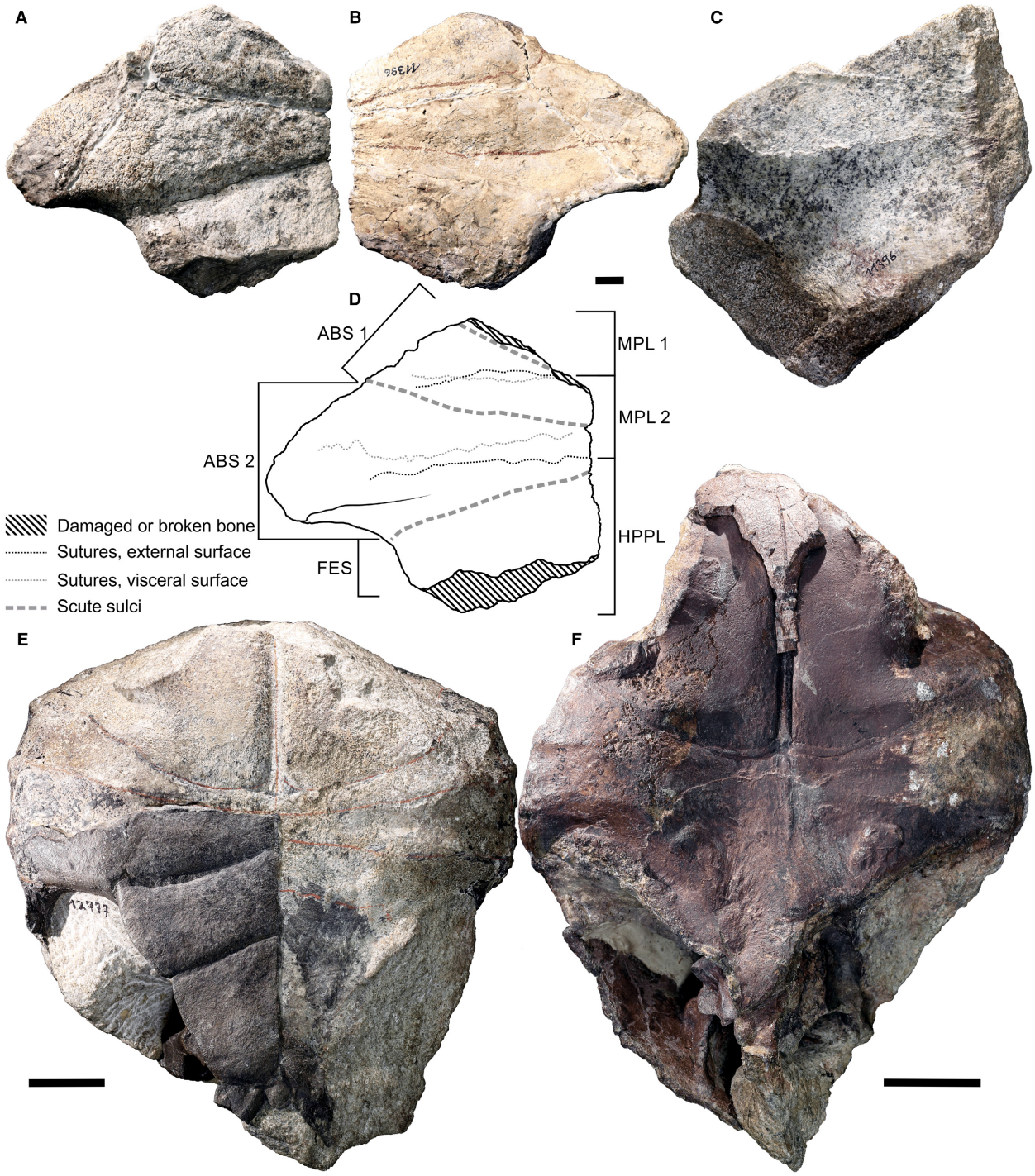

FIG. 7. *Proterochersis robusta*. A–D, SMNS 11396, right fragment of plastron in ventral (A, D) and visceral view (B), and natural cast of the visceral surface (C). E, SMNS 12777 (holotype) in ventral view. F, SMNS 16603 in ventral view. Note that the extent of the restored surface is not indicated, because it is difficult to evaluate, but it is minor in ventral view (A), and the natural cast (C) allows relatively accurate reconstruction of suture layout on the more extensively restored, visceral surface (B). *Abbreviations*: ABS, abdominal scute; FES, femoral scute; HPPL, hypoplastron; MPL, mesoplastron. Scale bars represent 1 cm (A–D); 5 cm (E, F). Colour online.

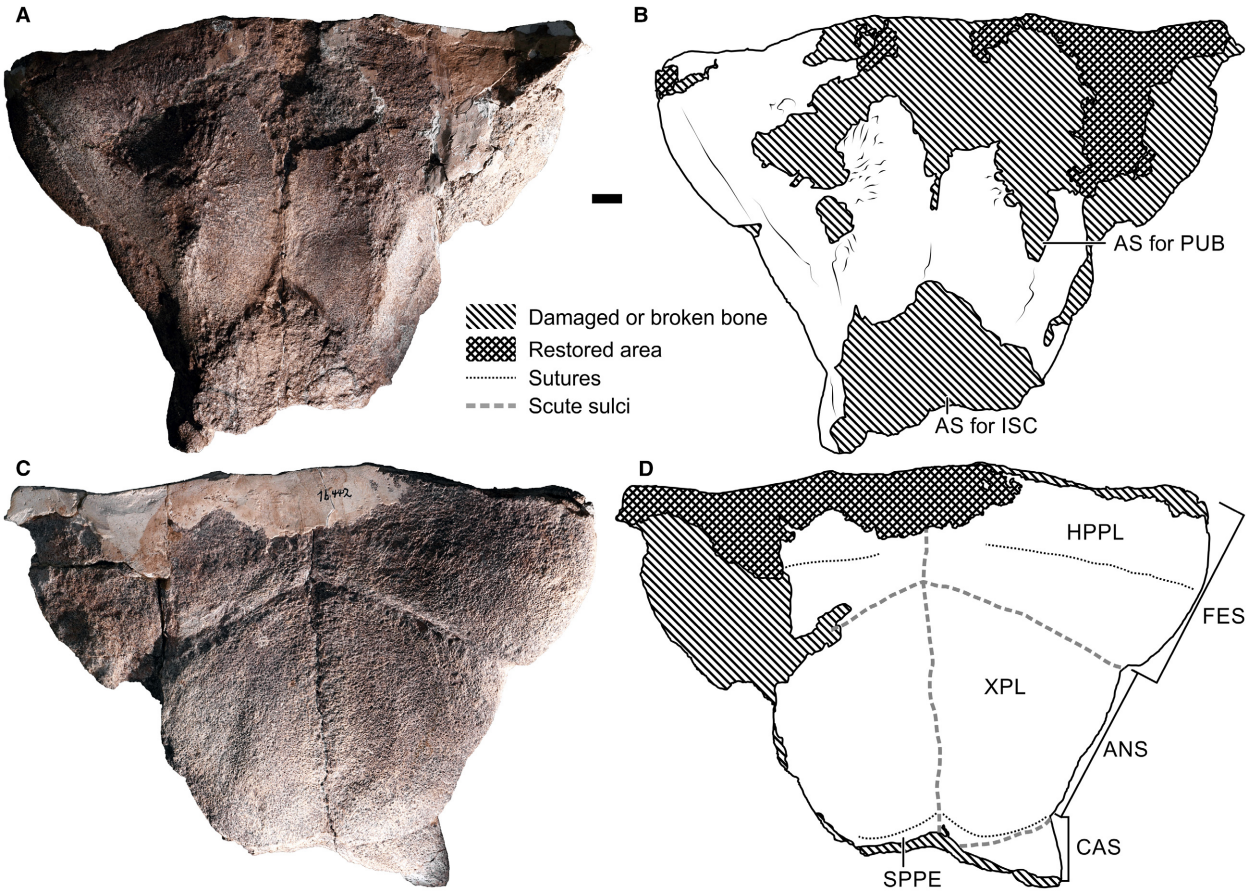

FIG. 8. *Proterochersis robusta*, SMNS 16442, posterior plastral lobe. A–B, visceral view. C–D, ventral view. *Abbreviations*: ANS, anal scute; AS, articulation site; CAS, caudal scute; FES, femoral scute; HPPL, hypoplastron; ISC, ischium; PUB, pubis; SPPE, supernumerary posterior plastral element (?hypoischium); XPL, xiphiplastron. Scale bar represents 1 cm. Colour online.

literature, as it was the case in the late nineteenth and early twentieth centuries.

Palaeochersis talampayensis *(Testudinata, Australochelyidae; Norian)*

Three specimens of *Palaeochersis talampayensis* (PULR 72, PULR 68, PULR 69) were described from the upper Los Colorados Formation in proximity of La Esquina, La Rioja Province, Argentina. Only PULR 68 (holotype) preserves shell remains.

Chinlechelys tenertesta *(Testudinata, ?Proterochersidae; Norian)*

Chinlechelys tenertesta was found in NMMNH locality 001 (Bull Canyon Formation), Quay County, New Mexico. It consists of a single specimen: NMMNH P-16697.

Joyce (2017) suggested the synonymy of the genera *Chinlechelys* and *Proganochelys* (based mostly on the similarity of the spiked osteoderm) creating a new combination: *Proganochelys tenertesta*. Just as in the case of *Keuperotesta limendorsa*, we find this attribution possible, but not unambiguously supported by available data. The only known specimen is very fragmentary and differs in some respects (shell thickness, shape of the femoral head) from all currently known specimens of *Proganochelys quenstedti* and *Prog. ruchae*. Additionally, it is separate geographically, being the only Triassic turtle known thus far from North America. Most importantly, however, it is nested separately from *Prog. quenstedti* in our phylogenetic analysis (see below), even despite its incompleteness (although with understandably low support). We therefore choose to use the original name, under which the specimen was described. We believe that merging it now with a known and well-recognized genus, with little data to support this (and thus a high risk of subsequent split when new specimens are available), may eventually create more taxonomic information noise in the literature, than sticking to the original name and possibly merging the taxa later, when data allow it. Furthermore, such merging may be confusing to non-palaeontologists, as evidenced by a recent paper of

Moustakas-Verho *et al.* (2017), who wrote 'One of the most basal known genera of turtles with a complete shell, *Proganochelys*, shows what appears to be ribs fused to metaplastic bone in the carapace'; an observation certainly not true for the genus *Proganochelys* as a whole.

Priscochelys hegnabrunnensis *(?Placodontia; Ladinian)*

The holotype and only known specimen of *Priscochelys hegnabrunnensis* (SMNS 80141) from the lower Ladinian, consists of a single bony plate with sulci visible on the external surface. It was found in Hegnabrunn, Germany. This specimen was described and figured by Karl (2005), Joyce & Karl (2006) and Scheyer (2008).

METHOD

The sutures were initially identified macroscopically and then confirmed (and for articulated specimens, traced) by careful examination using a binocular microscope. The macrophotographs of the specimen surface for Figures 12, 13, 16 and 17, and supplementary figures in Szczygielski & Sulej (2018*a*) were taken using Keyence Digital Microscope VHX-900F. The specimens SMNS 17755a and ZPAL V.39/22 were scanned using Nikon/Metris XT H 225 ST computed tomograph (500 ms exposition time, 1000 projections) housed in the Military University of Technology, Warsaw, Poland, and visualized using VGStudio MAX 2.1. ZPAL V.39/22 was scanned using 1 mm thick copper filter, 190 kV, 140 μA. SMNS 17755a was scanned using 2 mm thick copper filter, 205 kV, 100 μA. Based on the CT slices, a 3D volumetric rendering of ZPAL V.39/22 was produced using programs Fiji (Schindelin *et al.* 2012), Drishti 2.4.6 (Limaye 2012) and MeshLab 2016 (Cignoni *et al.* 2008). First, the contrast of CT slices was increased and the slice data were exported as raw files in Fiji. Then, from the exported data a triangulated mesh was generated and exported as a PLY file in Drishti. The final processing and scaling of the of the 3D models was done in MeshLab. To generate the interactive 3D PDF, the models were texturized and imported as OBJ files into DAZ Studio (https://www.daz3d.com/daz_studio) and then exported as U3D files. The U3D files were implemented into 3D PDF with Adobe Acrobat (https://acrobat.adobe.com).

For the phylogenetic analysis, we prepared a modified version of the matrix of Joyce *et al.* (2016) with updates by Pérez-García & Codrea (2018) and 13 new characters added, resulting in 257 characters. Three new taxa (*Pappochelys rosinae*, *Proterochersis porebensis* and *Chinlechelys tenertesta*) were added, and *C. tenertesta* was scored as three separate operational taxonomic units (OTU) differing in the scoring of the characters regarding the carapacial and osteoderm morphology: character 249 (carapacial dermal mosaic: 0 = present, at least in posterior region; 1 = absent, dermal ossifications reduced to peripheral and/or (supra)pygal rows or absent) and character 251 (spiky cervical osteoderms: 0 = absent; 1 = present). Variant A of *C. tenertesta* was scored treating the complex dermal spikes as cervical osteoderms (as proposed by Lucas *et al.* 2000; Joyce *et al.* 2009; char. 251 = 1) but the presence of the osteodermal mosaic anywhere else in the shell as unknown (char. 249 = ?). Variant B of *C. tenertesta* was scored as having both the complex osteoderms (char. 251 = 1) and the mosaic in the carapace (as suggested by Lichtig & Lucas 2015, 2016; char. 249 = 0). Variant C of *C. tenertesta* was scored treating the spikes as the posterior rim of the carapace (as discussed by Lucas *et al.* 2000 and preferred here; see text for discussion), thus the carapacial osteodermal mosaic is considered present (char. 249 = 0) and the presence of neck osteoderms is in that case unknown (char. 251 = ?). Considering the spikes as a part of the carapace allowed scoring the scutes as present (char. 108 = 0) and the posterior marginals as spiky (char. 256 = 1) for variant C of *C. tenertesta*. This amounts to 117 OTU in the matrix, but each variant of *C. tenertesta* was tested separately, by disabling the others.

Four traditional searches (Tree Bisection Reconnection, 1000 replications, 100 trees saved per replication; *Anthodon serrarius* Owen, 1876 as an outgroup) were performed using TNT (Goloboff *et al.* 2008) including: (1) *Chinlechelys tenertesta* variant A (variants B and C disabled); (2) *C. tenertesta* B (A and C disabled); (3) *C. tenertesta* C (A and B disabled); and (4) without *C. tenertesta* (variants A, B and C disabled). Characters 6, 18, 26, 38, 40, 47, 49, 56, 74, 75, 81, 86, 108, 109, 113, 118, 121, 124, 125, 126, 145, 146, 148, 163, 175, 198, 216, 217, 230, 244, 245, 248 and 252 were ordered (the character numbering starts with 0). The strict consensus was calculated for each analysis using the Consensus option and the common synapomorphies were found for all the most parsimonious trees in each analysis using the List Common Synapomorphies option of TNT. Jackknife resampling was performed using traditional search with 1000 replications (removal probability = 36). See Szczygielski & Sulej (2018*a*) for the matrix, character list, lists of synapomorphies and obtained trees, as well as for the representation of suture types.

SYSTEMATIC PALAEONTOLOGY

Family PROTEROCHERSIDAE Nopcsa, 1923

Diagnosis. Amended from Szczygielski & Sulej (2016). Five vertebrals wider than long, the first one semicircular anteriorly, with rounded posterior process invading the medial anterior area of the second vertebral; supramarginals and

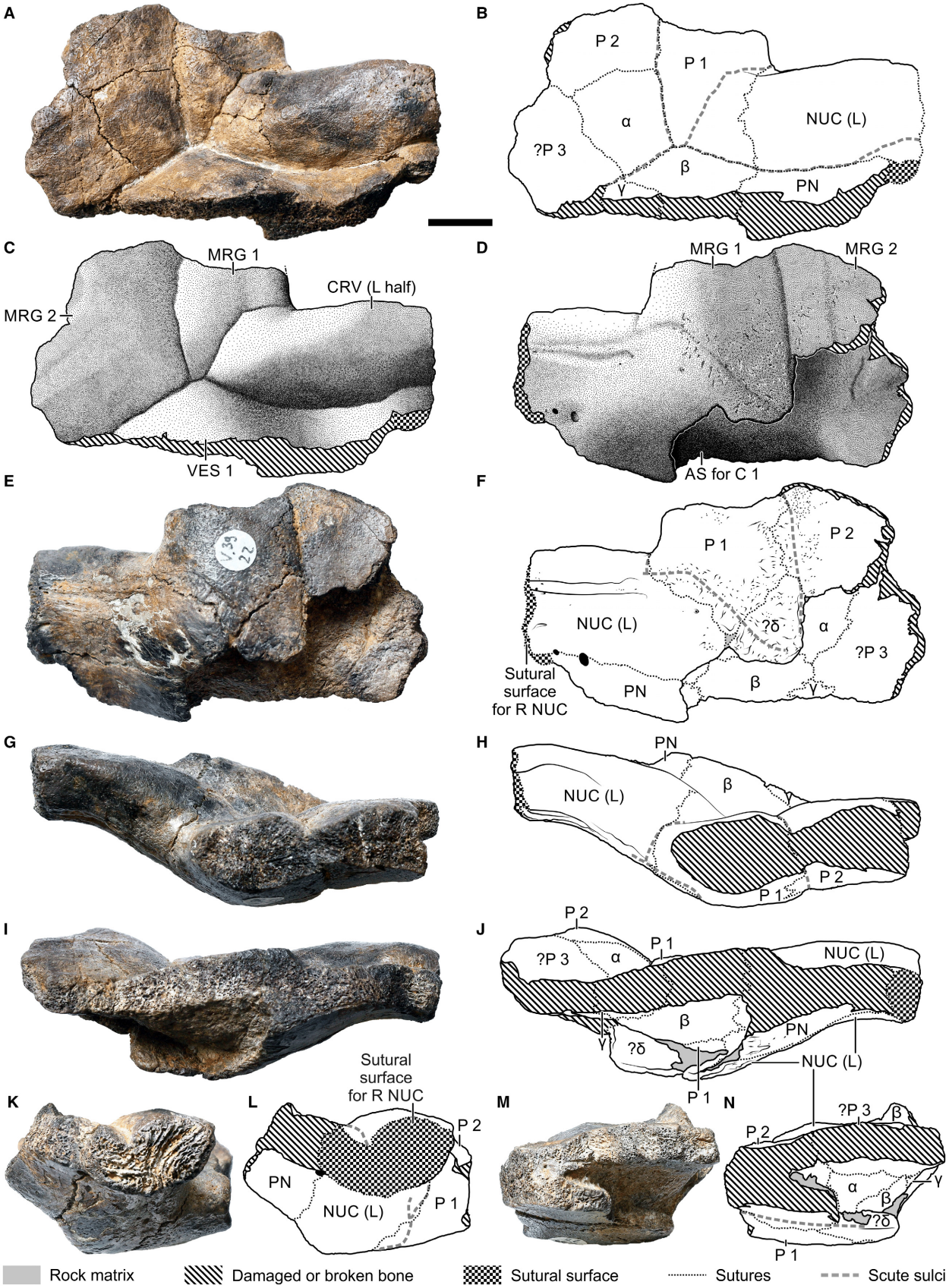

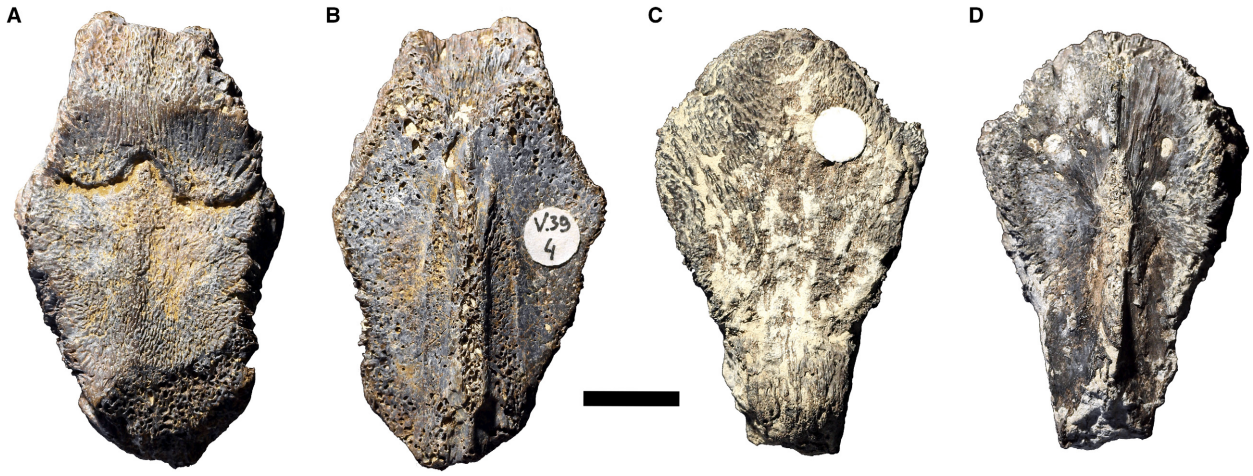

FIG. 10. *Proterochersis porebensis*, neurals. A–B, ZPAL V.39/4 in external (A) and visceral (B) view. C–D, ZPAL V.39/416 in external (C) and visceral (D) view. Scale bar represents 1 cm. Colour online.

inframarginals present; dorsal process of epiplastra large, not contacting the carapace; pelvis sutured to carapace and plastron; posterior process of ilium flattened dorsoventrally, fully attached to carapace; epipubic process long. More derived than *Odontochelys semitestacea* in having fully developed carapace with carapacial rim elements (peripherals, nuchal bone) and well-developed costals contacting each other suturally. Plesiomorphic regarding *Proganochelys quenstedti* in: two pairs of mesoplastra contacting at the midline; two pairs of abdominal scutes contacting at the midline; a bee wing-shaped coracoid; nuchale paired; additional dermal ossifications external to the first costal; posterior part of the carapace composed of a mosaic of numerous irregular dermal ossifications.

Genus PROTEROCHERSIS Fraas, 1913

Diagnosis. Amended from Szczygielski & Sulej (2016). Three pairs of supramarginals present; caudal notch present; paired extragular scutes divided by paired gulars; paired caudal scutes and the anal scute present in the posterior part of the plastron; three additional ossifications sutured posteriorly to ischium and xiphiplastra; sacral vertebrae fused or sutured to carapace. Plesiomorphic regarding *Proganochelys quenstedti* in having 11 dorsal vertebrae and the second pair of ribs forming fully developed costals. Differs from *Keuperotesta* in: dorsal surface of the carapace almost even; the eighth presacral vertebra being part of the dorsal region and co-ossified to the carapace and the following dorsal vertebrae (see discussion in Szczygielski 2017); anterior margin of the carapace, at most, moderately serrated; marginal series starting anterolaterally in relation to the cervical scute, contacting it widely; first vertebral scute contacting the first pleural anteromedially, rather than posteromedially.

Proterochersis robusta Fraas, 1913

Figures 1–8, 16N, 19; Szczygielski & Sulej (2018*a*, figs S1A–C, S3A, C; movies S1–S3).

Diagnosis. Amended from Szczygielski & Sulej (2016). Differs from *Proterochersis porebensis* in caudal notch semicircular, anterior margin of the carapace slightly serrated or undulated, shell high, costoperipheral sutures in the bridge region within the area of supramarginal scutes.

Occurrence. Proximity of Stuttgart, Baden-Württemberg, south-western Germany, Lower Löwenstein (Stubensandstein) Formation, middle Norian (Szczygielski & Sulej 2016 and references therein).

Remarks. Specimens from the Löwenstein Formation typically lack minute cracks, which are frequent (but not always present) in Triassic fossils (including those from the Trossingen, Grabowa and Los Colorados Formations)

FIG. 9. *Proterochersis porebensis*, ZPAL V.39/22, left half of the nuchal region of the carapace. A–C, dorsal view. D–F, ventral view. G–H, anterior view. I–J, posterior view. K–L, medial view. M–N, lateral view. *Abbreviations*: α, β, γ, δ, supernumerary ossifications; AS, articulation site; C, costal bone; CRV, cervical scute; L, left; MRG, marginal scute; NUC, nuchal bone; P, peripheral bone; PN, preneural bone; R, right; VES, vertebral scute. Scale bar represents 1 cm. Colour online.

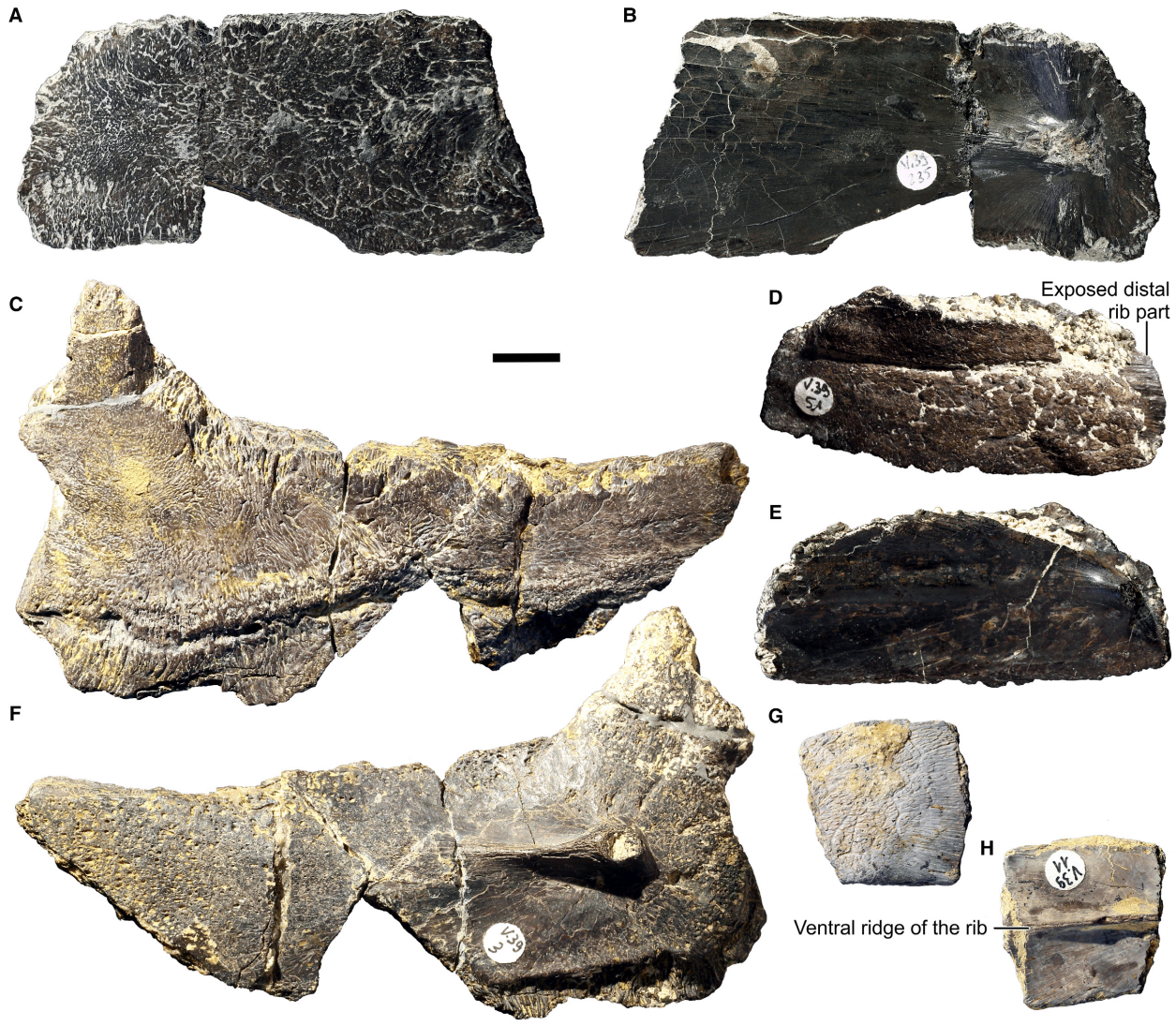

FIG. 11. *Proterochersis porebensis*, costal bones. A–B, ZPAL V.39/235 in external (A) and visceral (B) view. C, F, ZPAL V.39/3, right costal, in external (C) and visceral (F) view. D–E, ZPAL V.39/51, in external (D) and visceral (E) view. G–H, ZPAL V.39/11 in external (G) and visceral (H) view. Note that the ventral ridge of the rib may exhibit varied morphologies, from wide, low and quickly disappearing (B), through intermediate (E), to thin and pronounced (F, H). Scale bar represents 1 cm. Colour online.

and which may easily obscure any preserved sutures. Therefore, if present, sutures in these specimens are relatively unambiguous and easy to recognize with the help of optical equipment. Difficulties in suture tracing arise due to ankylosis (Pritchard 2008), which is common in Triassic turtles. Fortunately, several specimens of

FIG. 12. *Proterochersis porebensis*, evidence for supernumerary bones in the carapace. A–B, ZPAL V.39/20, proximal parts of two posterior right ribs in external (A) and visceral (B) view. C–D, ZPAL V.39/375, bony platelet with sutural edges in external (C) and visceral view (D). E–F, ZPAL V.39/373, bony platelet with sutural edges, a sulcus, and a tubercle in external (E) and visceral (F) view. G–H, ZPAL V.39/374, bony platelet with sutural edges and sulci in external (G) and visceral (H) view. I–J, ZPAL V.39/418, bony platelet with sutural edges and a sulcus in lateral (I) and medial (J) view. K–Q, ZPAL V.39/167, posterior left section of the carapace comprising of a single peripheral and four supernumerary ossifications (α, β, γ, δ) with sutural edges in lateral (K–L) and medial (M–N) view, a close-up of a suture in the area indicated by a rectangle in K (O), a close-up of sutures in the area indicated by a rectangle in K (P), and a 3D visualization of the surface of the same area (Q). R–W, ZPAL V.39/419, a fragmentary costal in dorsal (R), ventral (S), dorsoposterodistal (T–U), anterior (V) and distal (W) view; U and W are close-ups of the areas indicated in T. Note typical turtle characteristics of the bony platelets, such as straight and sinuous sulci (C, E, G, I) and tubercles (E), and visceral surface with vascular canals comparable with smooth surface in A. *Abbreviations*: MRG, marginal scute; P, peripheral bone; PLE, pleural scute; SLS, suture-like surface. Scale bar represents 1 cm. O–Q and U–W not to scale. Colour online.

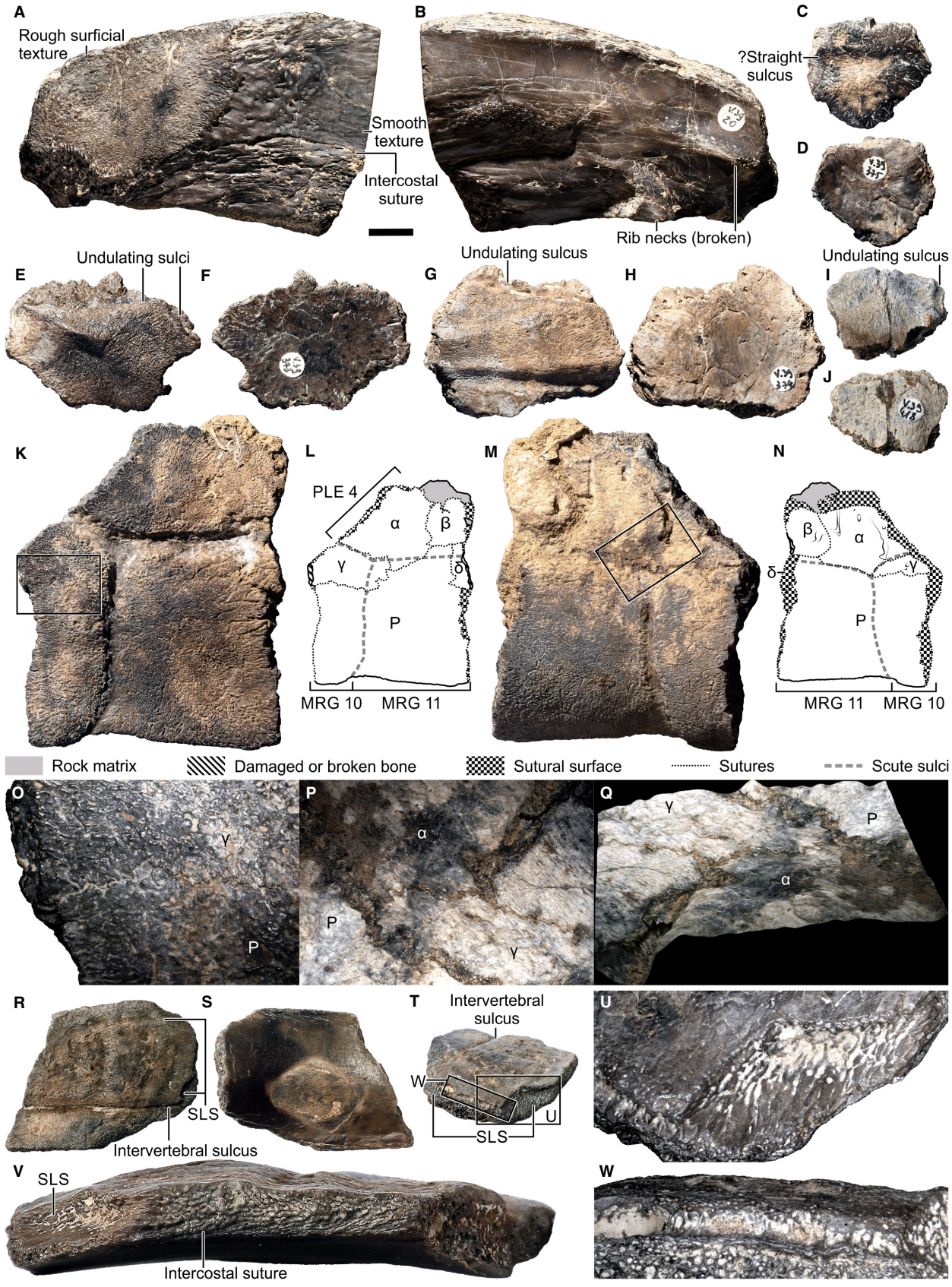

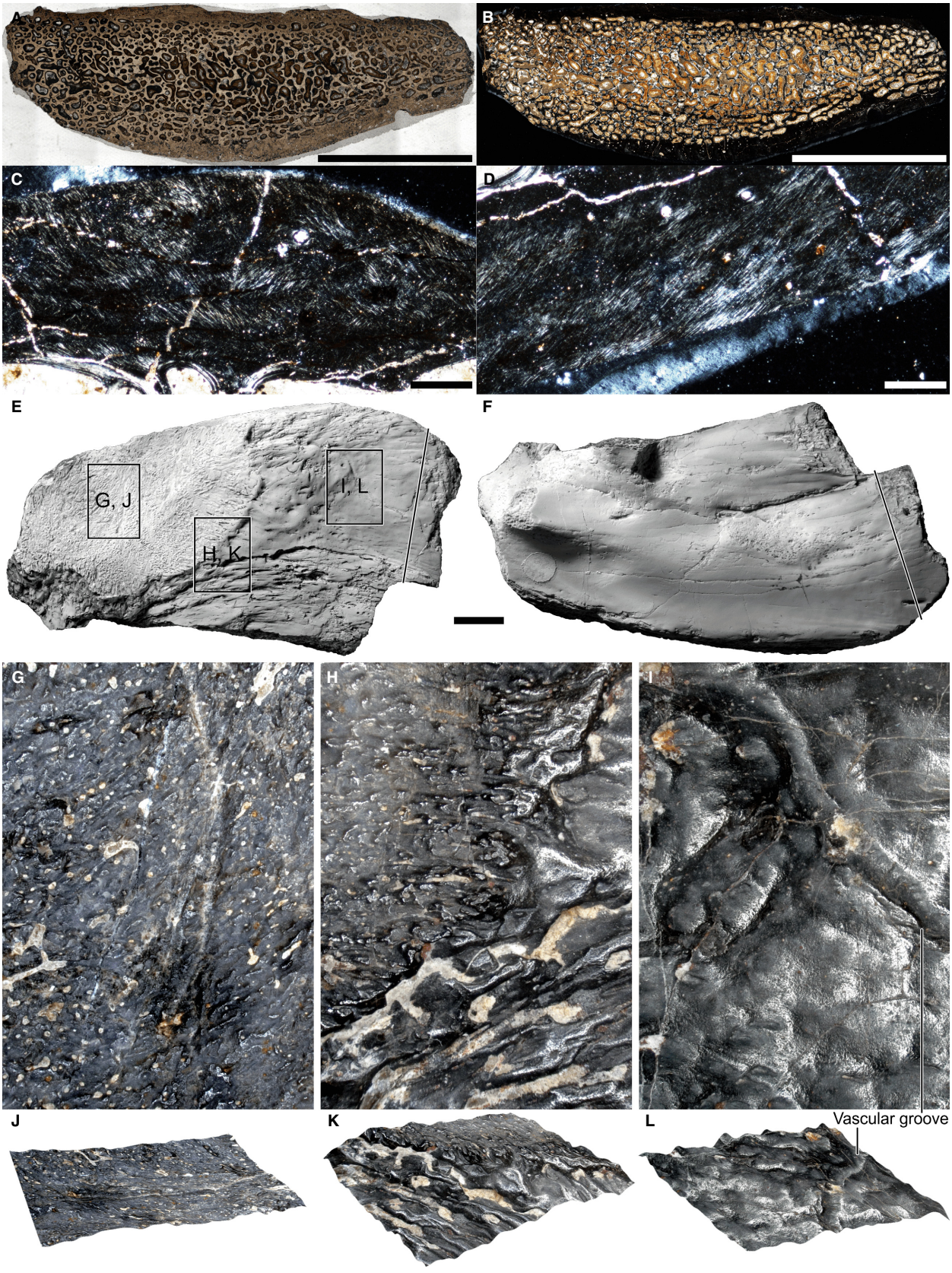

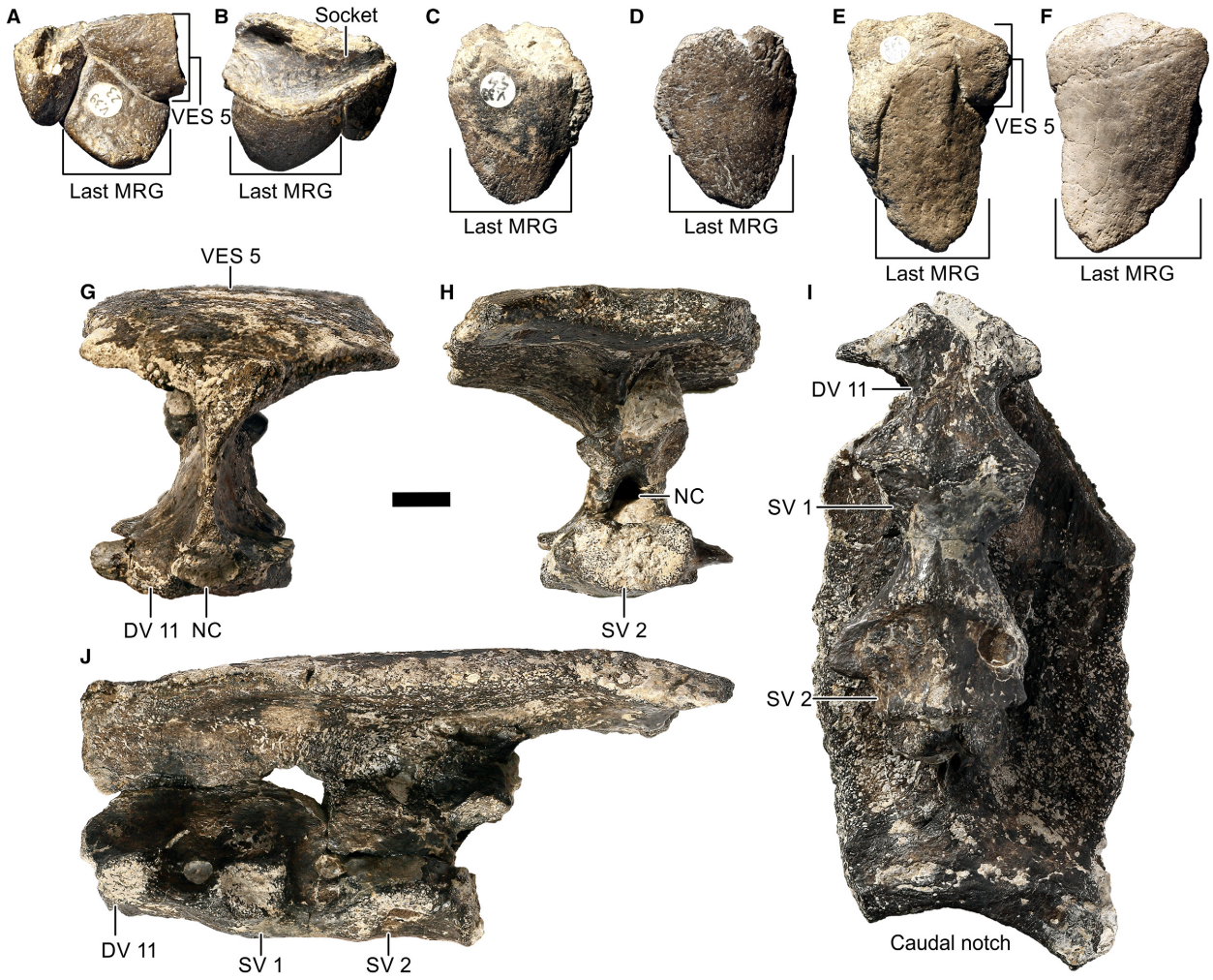

FIG. 14. *Proterochersis porebensis*, details of the pygal region of the shell. A–B, ZPAL V.39/23, left last peripheral in posterodorsal (A) and anteroventral (B) view. C–D, ZPAL V.39/54, right last peripheral in posterodorsal (C) and anteroventral (D) view. E–F, ZPAL V.39/213, left last peripheral in posterodorsal (E) and anteroventral (F) view. G–J, ZPAL V.39/402, middle section of the fifth vertebral scute area with attached the last dorsal and both sacral vertebrae in anterior (G), posterior (H), ventral (I) and lateral left (J) view. *Abbreviations*: DV, dorsal vertebra; MRG, marginal scute; NC, neural canal; SV, sacral vertebra; VES, vertebral scute. Scale bar represents 1 cm. Colour online.

Proterochersis robusta preserve sutures in some form, either as imprints on the surface of the internal moulds (e.g. the sutures between the hyo- and first pair of mesoplastra in SMNS 12777 and SMNS 16603), as thin lines of differently coloured matrix visible between the bony elements (e.g. the sutures between some of the elements of the anterior part of the carapace and between the xiphiplastron and posterior additional plastral

FIG. 13. *Proterochersis porebensis*, ZPAL V.39/20, proximal parts of two posterior right ribs, histology and details of external surface. A–B, histological section of the anterior costal in normal (A) and polarized light (B); anterior to the right; note well-developed cortexes. C, close-up of the external cortex in polarized light. D, close-up of the internal cortex (anterior part) in polarized light. E–F, whole specimen before sectioning in external (E) and visceral (F) view with approximate location of sections indicated. G, J, close-up (G) and 3D visualization (J) of the external surface in proximal part (indicated by a rectangle in E) exhibiting typical for *Proterochersis porebensis*, rugose texture indicative of ossification within external layers of dermis. H, K, close-up (H) and 3D visualization (K) of the external surface in middle part (indicated by a rectangle in E) showing transition between the elevated, normally textured proximal and depressed, smoother distal part. I, L, close-up (I) and 3D visualization (L) of the external surface in distal part (indicated by a rectangle in E) exhibiting atypical, smooth and wavy texture, perforated by vascular canals, typical for bones ossifying below or in deep layers of the dermis. Scale bars represent 1 cm (A, B, E, F); 1 mm (C–D). Colour online.

FIG. 15. *Proterochersis porebensis*, peripherals. A–C, ZPAL V.39/55, anterior or posterior peripheral in (?)dorsal (A), (?)ventral (B) and (?)anterior (C) view; see text for discussion. D–G, ZPAL V.39/14, bridge region peripheral in anterior (A), dorsal (B), ventral (F) and lateral (G) view. H–K, ZPAL V.39/173, posterior bridge region peripheral in dorsal (H), ventral (I), lateral (J) and medial (K) view. L–O, ZPAL V.39/181, right posterior peripheral in lateral (L), medial (M), posterior (N) and distal (O) view. *Abbreviations*: CPS, costoperipheral suture; MRG, marginal scute. Scale bar represents 1 cm. Colour online.

ossifications in SMNS 16442; the sutures between the dermal ossifications of SMNS 17755a; the sutures between the peripherals and costals in SMNS 17757; the costoperipheral sutures in SMNS 18440; the same mode of preservation is also present, e.g. in the skull of *Proganochelys quenstedti* SMNS 16980, see Szczygielski & Sulej 2018*a*, fig. S1D), or as more or less well-defined, three-dimensional surficial characters (e.g. the sutures between

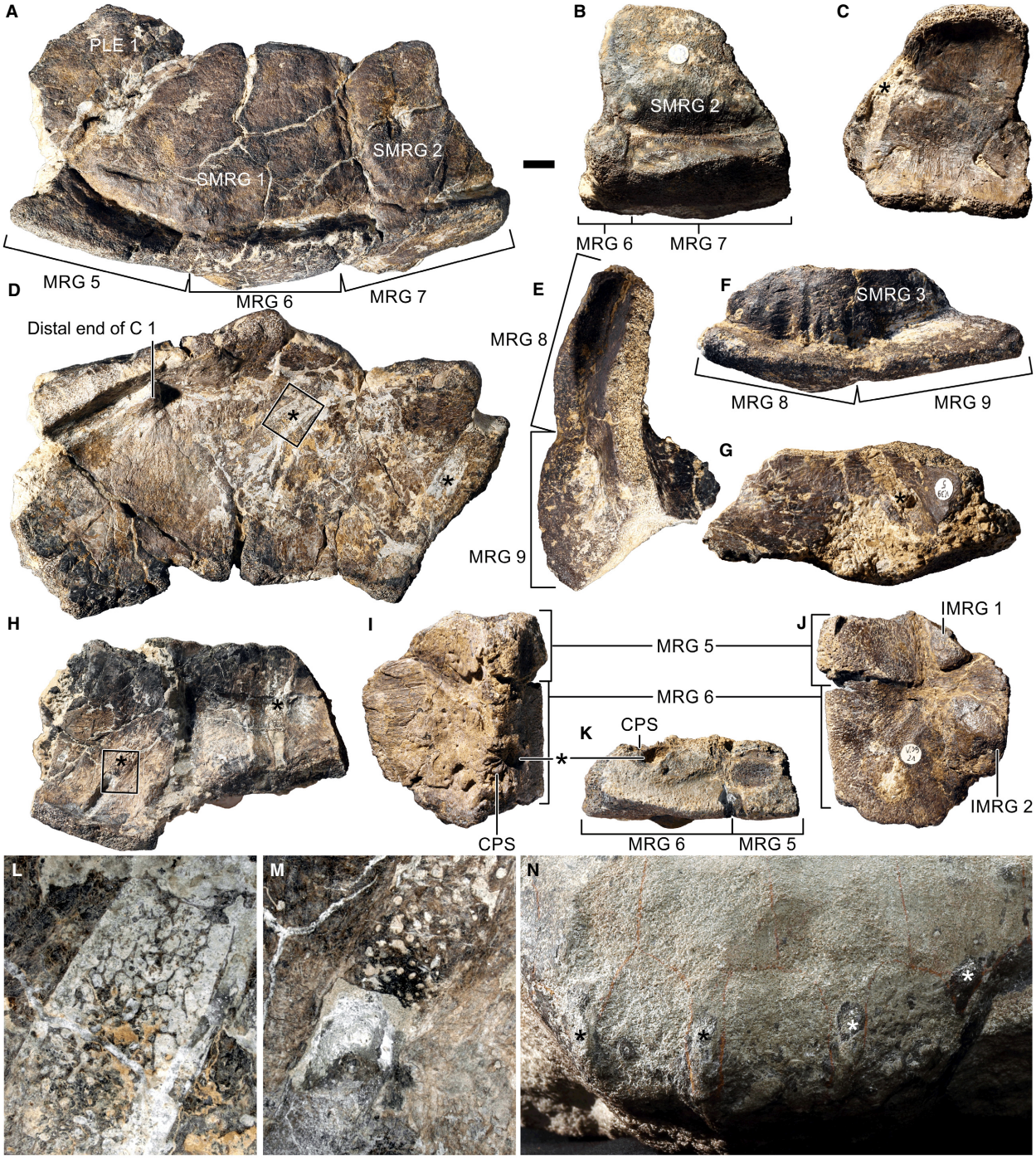

FIG. 16. *Proterochersis* spp., bridge region. A, D, L, *Proterochersis porebensis*, ZPAL V.39/8, anterior left section of the bridge in visceral (A) and lateral (D) view, and close-up of the area indicated by a rectangle in D (L). B–C, *Proterochersis porebensis*, ZPAL V.39/168, middle left section of the bridge in lateral (B) and visceral (C) view. E–G, *Proterochersis porebensis*, ZPAL V.39/5 posterior left section of the bridge in dorsal (E), lateral (F) and visceral (G) view. H, M, *Proterochersis porebensis*, ZPAL V.39/376, (?)middle left section of the bridge in visceral view (H) and close-up of the area indicated by a rectangle in H (M). I–K, *Proterochersis porebensis*, ZPAL V.39/21, anterior right section of the bridge in dorsal (I), ventral (J) and lateral (K) view. N, *Proterochersis robusta*, SMNS 12777 (holotype), left bridge area of the Steinkern in lateral view. Note distal sections of the ribs visible in visceral view partially as cancellous bone and partially as imprints (L–M and asterisks in C–D, G–I and K) and remaining inside the rock matrix of the Steinkern (asterisks in N). *Abbreviations*: C, costal bone; CPS, costoperipheral suture; IMRG, inframarginal scute; MRG, marginal scute; PLE, pleural scute; SMRG, supramarginal scute. Scale bar represents 1 cm. Colour online.

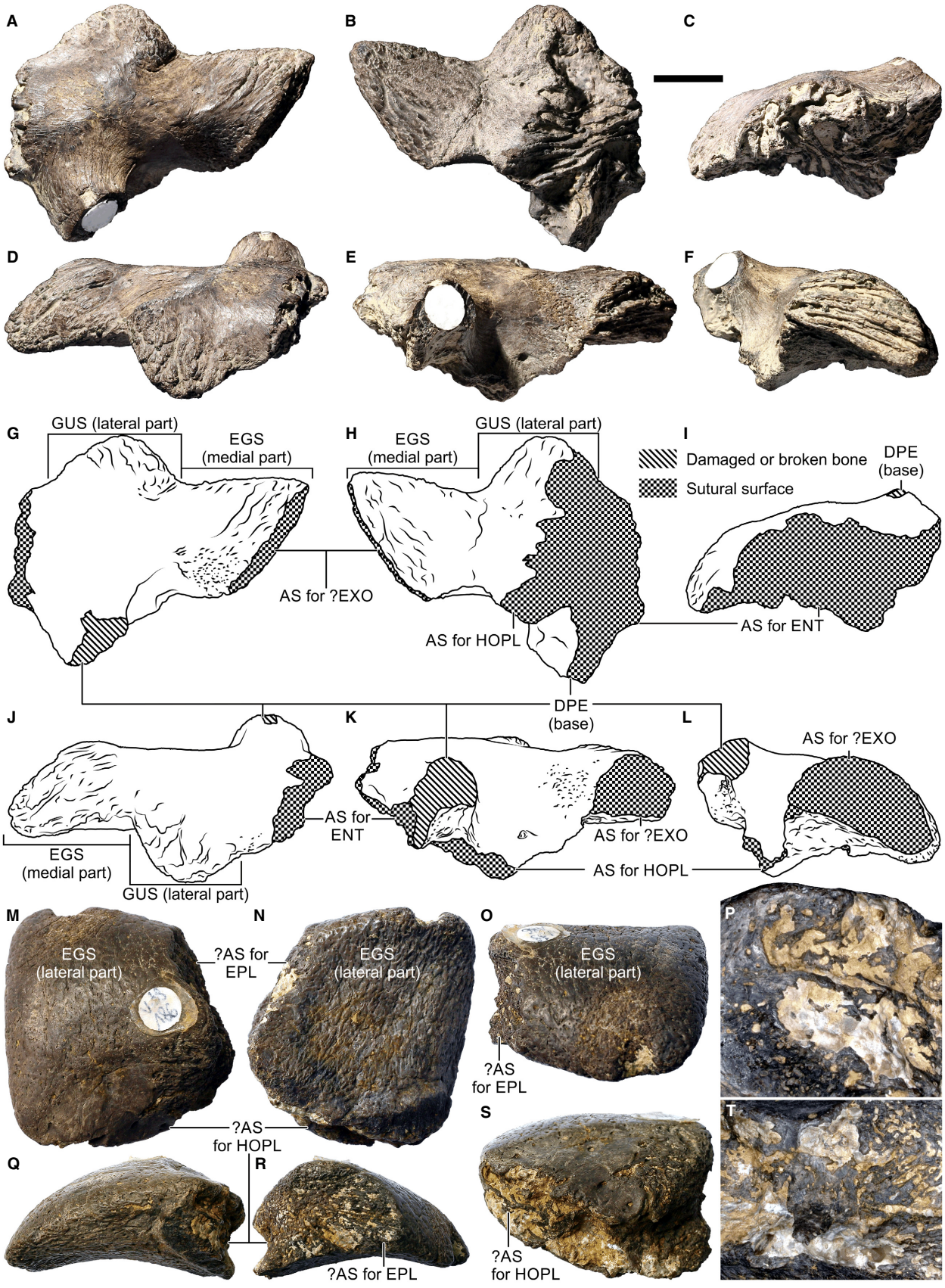

the first and second mesoplastron, and between the second mesoplastron and hypoplastron in SMNS 11396 and SMNS 18440; the sutures between the costals and peripherals, between the ento- and hyoplastra, and between the hypo- and xiphiplastra in SMNS 16442; the sutures between the hyo- and first mesoplastron, between the first and the second mesoplastron, between the second mesoplastron and hypoplastron, and between the hypo- and xiphiplastron in SMNS 17755). Disarticulation of elements along the sutures is rare in the Löwenstein Formation turtles, a special case being the anterior plastral lobe of SMNS 16442.

Description

Nuchal bone. None of the *Proterochersis robusta* specimens preserves sutures around the nuchal bone. SMNS 16442 is the only specimen of that species exhibiting sutures in the anterior part of the carapace, but contrary to our previous comments (Szczygielski & Sulej 2016) it lacks the cervical scute. Its anterior part corresponds to the area of the first vertebral scute, as indicated by radial grooves on its exterior surface, the posterior sulcus, and the relation of its anterior border to the scapular pits and the first pair of costals visible on the visceral surface (Fig. 1B, D). It is hard to say how closely the preserved edge follows the anterior sulcus of the first vertebral scute, but some erosion is highly probable.

Neurals and preneurals. The only *Proterochersis robusta* specimen showing any sutures around neurals is the badly damaged anterior part of the carapace of SMNS 16442 (Fig. 1). An anterior fragment of the second vertebral scute area is preserved in the middle part of that specimen. The posterior section of the specimen consists of the medial part of the third vertebral scute area. Viscerally, the damaged scapular pits are visible, as well as the medial parts of the first pair of costals and broken neural spines of the vertebrae. Historically, it was attempted to trace the layout of the sutures, as evidenced by pencil markings on the bone surface, but careful examination of the specimen using a binocular microscope allowed for convincing validation of only some of these (Fig. 1C) and partial outlines of what seem to be two preneurals and two or three neurals. We interpret the former two elements as preneurals based on their position relative to the first dorsal vertebra (the posterior suture of the second preneural is located just anterior to the base of the neural process of the first dorsal vertebra) and comparison with the *Prot. porebensis* specimen ZPAL V.39/22 (the nuchal in that specimen does not enter the area of the first neural). The preneurals are wider than long; the first one is pentagonal, with a small, triangular posterior process; the second one is fan-shaped. The two anterior neurals are hexagonal, coffin-shaped; the shape of the third one is difficult to estimate. The first neural is wider than long, the remaining two longer then wide. It must be kept in mind that this specimen is eroded and broken, and the interpretation of the elements visible there (particularly the preneurals) must be taken with caution.

Dermal carapacial mosaic. Several specimens of *Proterochersis robusta* exhibit sutures delineating the dermal bones of the carapace, and a larger than usual number of these elements is apparent, particularly in the anterior (nuchal) and the posterior (pygal) region of the carapace, where an irregular mosaic of bones (here termed the osteodermal carapacial mosaic) is present. There seems to be no clear qualitative distinction between these bones and peripherals; we therefore use the term 'peripherals' on topological basis, referring to the dermal bones located in the apical parts of marginal scute areas.

There are several sutures discernible running parallel to the anterior and anterolateral edge of the anterior carapacial part of SMNS 16442 and several running radially (at least one of them located in front of the first costal and thus delineating a dermal ossification present between the costal and the preneural). The sutures around the periphery of that specimen at first bring to mind the layout of peripherals, but they probably do not represent the peripherals, as defined above. Their position and inclination at the lateral region of the vertebral scutes does not correspond with the rim of the complete carapace (the peripherals would have to be very elongated, strap-like, directed heavily medially and cross the whole area of the first pleural) and the peripherals in *Proterochersis porebensis* do not enter the area of the first vertebral scute (see description of *Prot. porebensis*). Once again, however, the apparent sutures are often interrupted or dubious, and difficult to interpret. No sutures are discernible on the visceral surface.

The layout of the bones in the anterolateral marginal carapacial region of SMNS 16442 (Fig. 3) is complex and difficult to interpret. A set of ossifications of the marginal part probably represents the distal part of the first and the second costal, and five peripherals, with possible fragments of another two, but the layout of sutures is irregular, some of them are interrupted, and the destroyed external surface makes orienting the specimen problematic.

SMNS 17755a (Fig. 2; Szczygielski & Sulej 2018*a*, fig. S1A–C, movies S1–3) represents the left part of the posterior section of

FIG. 17. *Proterochersis porebensis*, anterior plastral bones. A–L, ZPAL V.39/404, isolated right epiplastron in dorsal (A, G), ventral (B, H), medial (C, I), anterior (D, J), posterior (E, K) and lateral (F, L) view. M–T, ZPAL V.39/186, probable isolated left supernumerary (extragular) ossification in dorsal (M), ventral (N), anterior (O), posterior (P, S–T), lateral (Q) and medial (R) view. P and T are close-ups of the posterior surface of the specimen, showing rounded, unbroken edges (P, T), suture-like lamellae (P) and an undamaged cortical bone (T) suggesting that the specimen is a separate element and not a part of a hyoplastron. The medial surface shown in R is damaged but exhibits a longitudinally lamellar, suture-like pattern comparable to the lateral surface of ZPAL V.39/404 (compare with F). *Abbreviations*: AS, articulation site; DPE, dorsal process of epiplastron; EGS, extragular scute; ENT, entoplastron; EPL, epiplastron; EXO, supernumerary (extragular) ossification; GUS, gular scute; HOPL, hyoplastron. Scale bar represents 1 cm. Colour online.

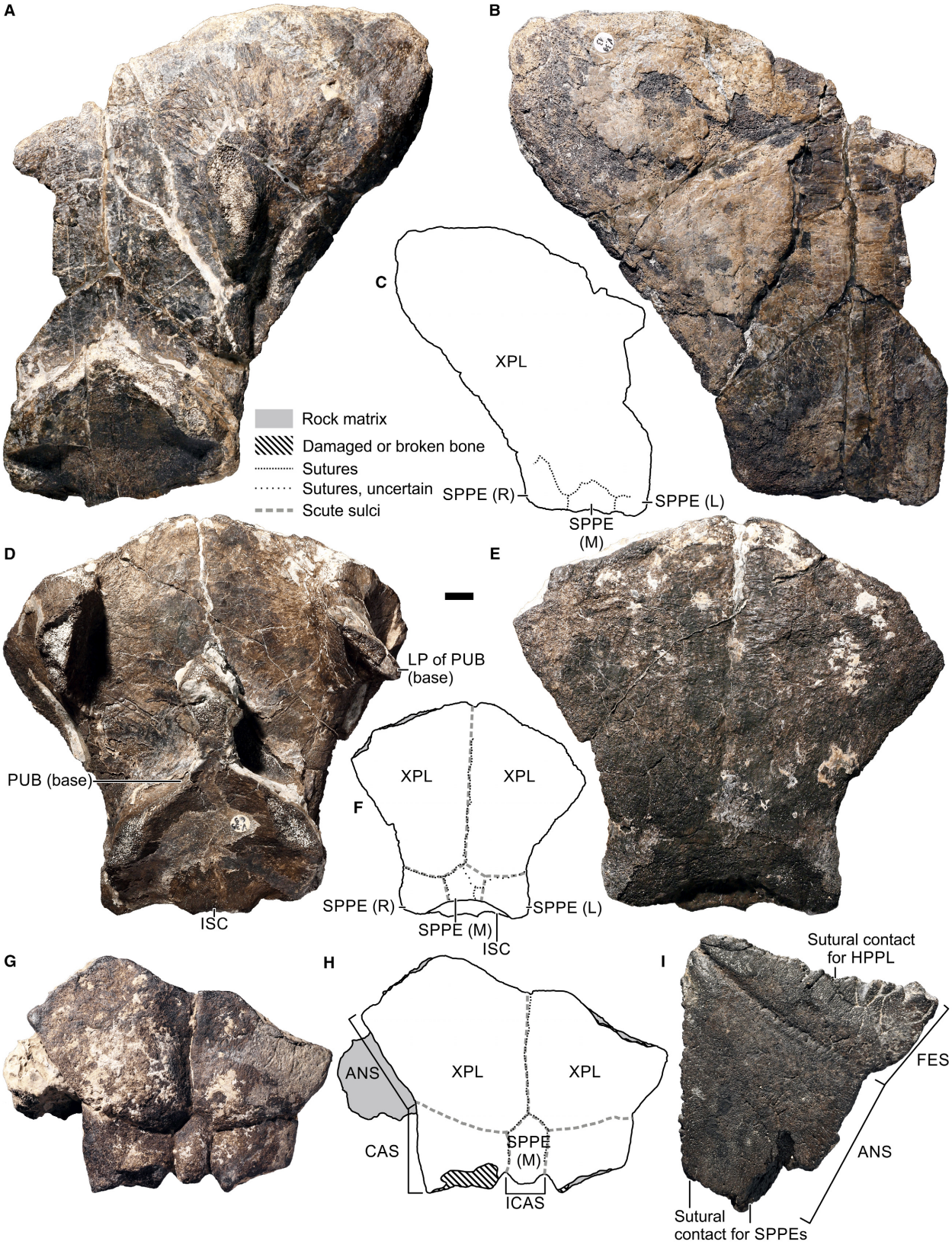

a *Proterochersis robusta* carapace. The layout of sulci leaves no doubt about its taxonomic and anatomical identity (see below), but the layout and number of ossifications is very different to that of any other turtle, with exception of the secondary armour of leatherback turtles. The entire surface of this specimen is covered in a complex pattern of sutures, revealing its origin as a mosaic of polygonal bones. They have serrated, interdigitating edges, which are typical for sutures (Szczygielski & Sulej 2018*a*, fig. S1) and easily distinguishable from the break surfaces (Szczygielski & Sulej 2018*a*, fig. S1C). A lack of disturbance and relocation (except for the posterodorsal region of the specimen, which is broken and collapsed) and the overall arrangement of the sutures indicate that the observed morphology is not an effect of any damage. The ossifications are irregular in shape, size and position, and exhibit more or less radial vascularization. Only in the upper parts of pleurals, most notably the third one, are there larger patches without visible sutures. It is possible that in these parts proper costals are exposed, although comparison with some specimens of *Prot. porebensis* (most notably, ZPAL V.39/20 and ZPAL V.39/373, see below) suggests the presence of dermal platelets in this area. The CT scans (Fig. 2E–G; Szczygielski & Sulej 2018*a*, movies S1–S3) clearly show the layout of the sutures in the lateral part of the specimen and a thickness of between approximately 0.4 and 1.5 cm (Szczygielski & Sulej 2018*a*, movies S1–S3). We were unable, however, to obtain a clear CT picture of the vertebral scute area (posterodorsal part) due to insufficient contrast between the bone tissue and the rock matrix, possibly because of some diagenetic changes in that region. The layout of the sutures, as seen on the surface, is laterally asymmetrical on the vertebral scute area. Unlike more derived turtles, but as in *Prot. porebensis*, the sutures between the elements tend to run along the scute sulci. Two elongate, flat bones stretch dorsoventrally below the mosaic and in part articulate with its visceral surface (Fig. 2G; Szczygielski & Sulej 2018*a*, movies S1–S3). They are most likely to be distal sections of ribs. Similar free rib apices are also preserved in the bridge area of SMNS 12777 (Fig. 16N) and CSMM specimen (see below), although the structures in SMNS 17755a are flatter and more costal-like (compare with ZPAL V.39/20; Figs 12A–B, 13, and see description below). They are partially disarticulated in that specimen, but in life they apparently contacted each other anteroposteriorly, at least in the dorsal part. We find it unlikely that they represent broken and relocated sections of the carapace, because of their elongate shape, uniform broadness, the same general dorsoventral and anteroposterior (rather than fully random) orientation, and good alignment with overlying dermal mosaic (they seem to fit well into gentle depressions visible in the visceral surface of the mosaic). Along the marginal border there runs a row of roughly rectangular elements that are positionally comparable to peripherals and probably are homologous to them. The supernumerary bones dorsomedial to the supposed peripherals of SMNS 17755a lack clear homology with carapacial bones of derived turtles, in which the caudal region of the carapace is composed only of costals, peripherals and a midline row of neurals, suprapygal(s) and pygal.

Bridge. Hyo-, meso- and hypoplastra participate in the bridge. Although this region is partially preserved as a bone in three suture-bearing specimens (SMNS 16442, Fig. 3; SMNS 17755, Fig. 4; and SMNS 18440, Fig. 5), the state of preservation makes it impossible to see the details of the bony connections clearly. The external surface of SMNS 16442 is badly eroded so it is difficult to see any sulci, with exception of one fragment of a longitudinal and wavy sulcus located in the anterior part of the specimen, probably dividing the first pleural and the fourth marginal. The plastral surface of SMNS 17755 is well-preserved, but the lateral surface of the peripherals and costals is also damaged (although at least identifiable). Out of these three specimens, SMNS 18440 is the best preserved. In all three cases, some costoperipheral, interperipheral and intercostal sutures are preserved, but they are frequently interrupted, sometimes dubious, and often difficult to interpret.

From what can be said, based on SMNS 17755 (Fig. 4) and SMNS 18440 (Fig. 5), the costoperipheral sulci at the bridge region are located just ventral to the middle of the supramarginals, so the ventral parts of these scutes were supported by the peripherals, and the dorsal parts by costals. Three unambiguous intercostal sutures are visible: one around the anterior third of the first supramarginal (possibly the suture between the first and the second costal; Fig. 5E, F), one at the middle of the second supramarginal (dividing the second and the third costal; Fig. 5E, F) and one around the anterior third of the third supramarginal (dividing the third and fourth costals; Figs 4E–F, 5E–F). Slightly cranial to the posterior sulcus of the ninth marginal there is another suture (Figs 4E–F, 5E–F) probably dividing the fifth and sixth costals, although this region is fragmentarily preserved and close to the mosaic-filled area preserved in SMNS 17755a (Fig. 2), so the interpretation of the elements is uncertain. Four interperipheral sutures are identifiable: one at the level of the sulcus between the fifth and the sixth marginal scute (Fig. 5E, F), one at the level of the second mentioned intercostal suture (at the middle of the second supramarginal, Fig. 5A, B, E, F), one slightly posterior to the third mentioned intercostal suture (near the middle of the third supramarginal; Fig. 5A, B, E, F) and one at the level of (in SMNS 17755, Fig. 4E–F) or slightly anterior to (in SMNS 18440, Fig. 5C–D, E–F) the ambiguous fourth of the mentioned intercostal sutures (near the posterior sulcus of the ninth marginal). Apparently, the peripherals were external to the plastral bones and costals and supported at least most of the inframarginals (clearly visible, e.g. in the last inframarginal of SMNS 18440, Fig. 5C–D).

The layout of the distal ends of the dorsal ribs is unusual in relation to the peripherals in the bridge region, best exhibited by

FIG. 18. *Proterochersis porebensis*, posterior plastral lobes. A–C, ZPAL V.39/13 in visceral (A) and ventral (B–C) view. D–F, ZPAL V.39/69 in visceral (D) and ventral (E–F) view. G–H, ZPAL V.39/68 in ventral view. I, ZPAL V.39/170, isolated left xiphiplastron in ventral view. Damaged or broken bone not indicated in C due to extensive surficial damage. *Abbreviations*: ANS, anal scute; CAS, caudal scute; FES, femoral scute; HPPL, hypoplastron; ICAS, intercaudal scute; ISC, ischium; L, left; LP, lateral process; M, medial; PUB, pubis; R, right; SPPE, supernumerary posterior plastral element (?hypoischium); XPL, xiphiplastron. Scale bar represents 1 cm. C and F not to scale. Colour online.

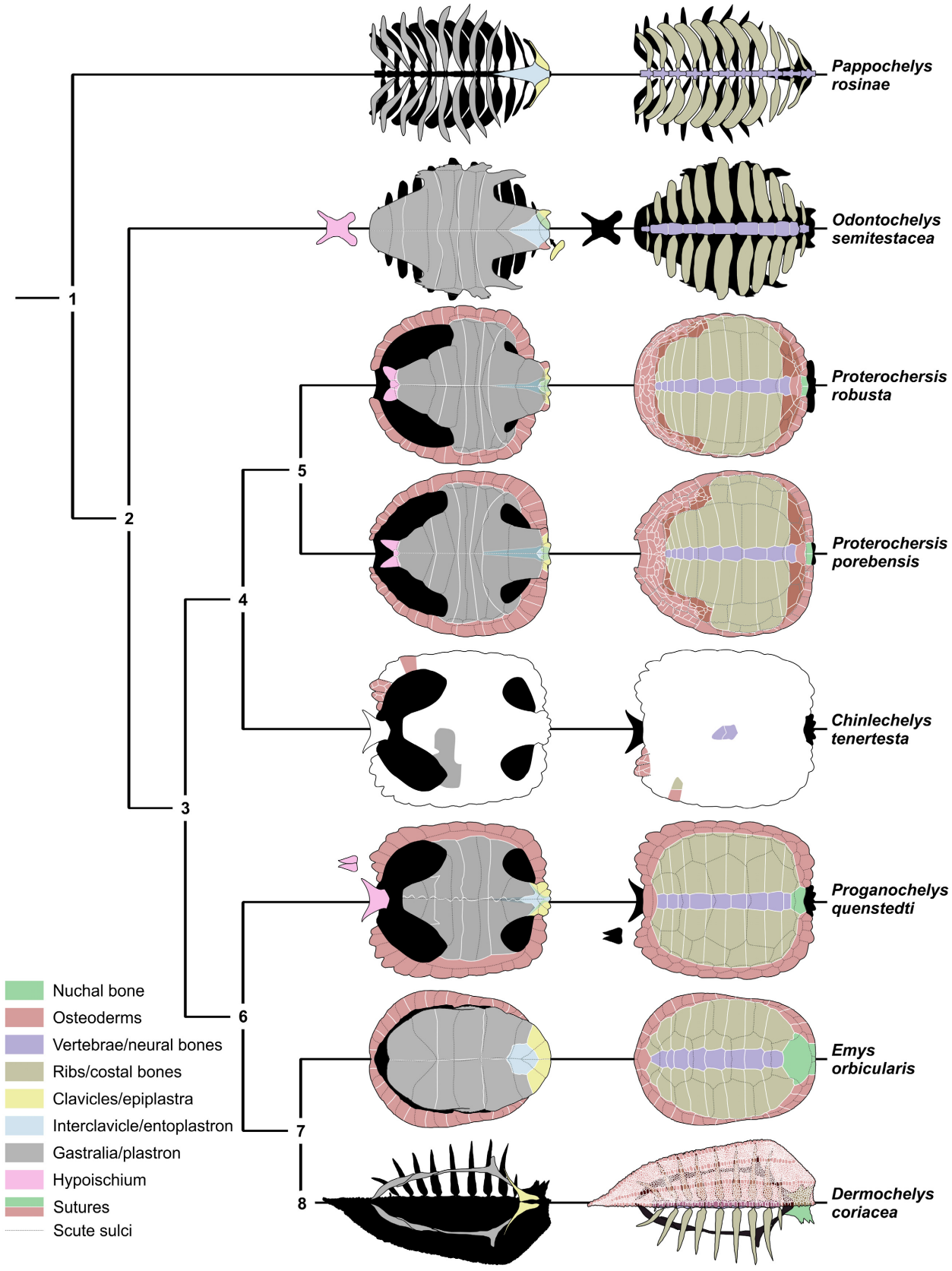

SMNS 12777 (Fig. 16N), but also seen in the CSMM specimen and *Proterochersis porebensis* (see below). The apical parts of the ribs in some specimens were apparently free from peripherals, protruded viscerally, along the body wall, and are still present in the steinkerns of SMNS 12777 and the CSMM specimen. This was apparently noticed by Fraas (1913), but ignored by later researchers.

Plastron. The sutures between the plastral elements are the easiest to discern, especially on the visceral surfaces of the plastron, because there they are not obscured by the coarse vascular bone ornamentation, which is present externally. Generally, the layout of sutures in the plastron of *Proterochersis* spp. observed by us agrees with the pattern presented for *Prot. robusta* by Gaffney (1990).

Entoplastron. As shown by SMNS 16442, the entoplastron in ventral view is relatively small and V-shaped or cordiform (Fig. 6), with small paired angulated anterior processes and a medial notch cranially. Its anterior half was covered by the medial part of the gular scutes, and the posterior half by the craniomedial parts of the humeral scutes; the sulci delimitating these four scutes meet in the middle of the ventrally exposed part of the entoplastron. Viscerally, the exposed area of the entoplastron is much larger, with an elongated posterior process (which is incomplete posteriorly in SMNS 16442, but visible as an impression in SMNS 12777 and SMNS 16603; Fig. 7E, F). Medially, just behind the notch dividing the processes supporting gular scutes, there is an eminence on the visceral side of the entoplastron, which projects posteriorly into the posterior process of epiplastron. Laterally to this eminence, the entoplastron slopes downwards and forms triangular fields (wider anteriorly, and gradually thinning out posteriorly) approximating the level of the visceral surface of hyoplastra. The epiplastra articulated craniolaterodorsally with the entoplastron, and apparently did not meet (or met only barely) at the midline.

Hyoplastra. The hyoplastra articulate ventroposterolaterally with the anterior part of the entoplastron, and ventrally with the posterior process of entoplastron. The anterior limit of the hyoplastra was at the level of, or just behind, the sulcus between the extragular and humeral scutes. The humeropectoral sulcus is located around their middle part. The suture between the hyoplastra and the first pair of mesoplastra is usually anchor-shaped and accentuated by the ridge on the visceral surface, as in SMNS 12777 (Fig. 7E), SMNS 16603 (Fig. 7F) and *Proterochersis porebensis* (see Szczygielski & Sulej 2016), but seems to be smooth in SMNS 17755 (Fig. 4), possibly due to imperfect ossification of the plastral bones in that specimen. It falls just before the sulcus between the pectoral and the first abdominal scute, in some specimens intersecting it.

Mesoplastra. Both the first and the second mesoplastra are approximately rectangular medially, but the second one slightly broadens laterally, resulting in a somewhat diverging layout of its sutures. Their posterior sutures are located around the middle of the first and the second abdominal scute, respectively. They are best visible in SMNS 17755 (Fig. 4) and SMNS 18440 (Fig. 5).

Xiphiplastra. The suture between the hypo- and xiphiplastron is located slightly posterior to the middle of the femoral scute, and is much less obvious than the other plastral sutures. This region is just anterior to the point of contact of the lateral pubic processes, and is therefore usually missing (broken off with the pelvis), damaged (due to pelvis breaking off) or the suture is obliterated by bone remodelling. It is best visible on the external surface of SMNS 16442 (Fig. 8).

When observed under a binocular microscope, in the posterior region of the anal scute area of SMNS 16442 (Fig. 8), a faint remnant of the suture can be found, which we interpret as a point of contact between the xiphiplastron and posterior plastral ossifications (possibly homologous to hypoischium, see *Proterochersis porebensis* below). Unlike most of the plastral sutures of *Proterochersis robusta*, it is not transverse, but V-shaped, with the point turned cranially, and the arms gently bowed caudally.

FIG. 19. Phylogeny (topology based on the analysis performed herein utilizing the *Chinlechelys tenertesta* scoring variant C; complex spikes treated as the posterior part of the shell, as pictured, and shell mosaic present) and reconstructions of trunk body sections (ventral (left row) and dorsal (right row) view) of turtles and stem turtles discussed in the text. Bones are semi-transparent to show structures not exposed externally. Approximate layout of shell sutures is represented by white lines. Where data was missing, the shell suture layout of *Proterochersis robusta* and *Prot. porebensis* was reconstructed by analogy with each other or (if needed) other Triassic taxa. 1, Pantestudinata: carapacial ridge, broad ribs, gastralia merging; 2, neuralia, plastral scutes, gastralia fused into plastral bones; 3, Testudinata: carapacial scutes, cleithra incorporated into the carapace as an (?initially paired) nuchal bone, ten pairs of costal bones, intervertebral articulation of ribs, shell consolidated; 4, (?)carapacial dermal mosaic present; 5, Proterochersidae: (?)hypoischium sutured to plastron; 6, first dorsal vertebra shifting to cervical, nine pairs of costals, nine neurals, one pair of abdominal scutes, one pair of mesoplastra; 7, Testudines: eight pairs of costals, eight neurals, dorsal epiplastral processes reduced, mesoplastra reduced, hypoischium lost; 8, *Dermochelys coriacea*: shell reduced, entoplastron lost, secondary dermal carapacial mosaic present. The layout of the anterior plastral elements in *Odontochelys semitestacea* is controversial, we present two interpretations: the right side is based on Lyson *et al.* (2014) and the left side on Nagashima *et al.* (2013*b*). For the current dataset, the carapacial osteodermal mosaic may be an autapormophy of Proterochersidae + *C. tenertesta* (4), but see text for discussion. Both known variants of *Prog. quenstedti* hypoischium are shown. The posterior plastral ossifications are coloured as a hypoischium in *Proterochersis* spp. following the hypothesis proposed herein, but alternatively they may be neomorphic or serially homologous to gastral-derived plastral bones. Note that no data are available for on bone composition of the carapace margin (nuchal, peripherals, etc.) of *Proganochelys quenstedti*. The earliest evidence of a single nuchal bone is known from the Jurassic. See text for discussion.

Proterochersis porebensis Szczygielski & Sulej, 2016
Figures 9–15, 16A–M, 17–19; Szczygielski & Sulej (2018*a*, figs S2, S4C–H, movies S4–S7, models S1–S2)

Diagnosis. Amended from Szczygielski & Sulej (2016). Articular surface of femoral head triangular in dorsal view. Differs from *Proterochersis robusta* in caudal notch triangular, anterior margin of the carapace nearly straight, anterior edge of the third marginal only slightly rounded, lower shell, costoperipheral sutures in the bridge region at the level of the sulcus between the marginals and supramarginals. Differs from *Keuperotesta limendorsa* in acromion and coracoid forming an angle of ~120°.

Occurrence. Proximity of Poręba, Silesian Voivodship, southern Poland, lower part of Patoka Member of the Grabowa Formation (formerly Zbąszynek Beds), middle Norian (Szulc *et al.* 2015; Szczygielski & Sulej (2016) and references therein).

Remarks. There are only a few specimens of *Proterochersis porebensis* with sutures visible. Large specimens appear to be fully ankylosed and their surface is usually cracked, preventing unambiguous identification of any remaining sutures. Fortunately, several fragmentary specimens lack surface cracking and either exhibit well-preserved sutures (ZPAL V.39/20, ZPAL V.39/22 and ZPAL V.39/167, but also ZPAL V.39/13, ZPAL V.39/68, ZPAL V.39/69 and ZPAL V.39/213) or are preserved as disarticulated bones with at least some sutural edges (ZPAL V.39/4, ZPAL V.39/14, ZPAL V.39/21, ZPAL V.39/23, ZPAL V.39/54, ZPAL V.39/55, ZPAL V.39/170, ZPAL V.39/173, ZPAL V.39/181, ZPAL V.39/373, ZPAL V.39/374, ZPAL V.39/375, ZPAL V.39/404, ZPAL V.39/416, ZPAL V.39/417, ZPAL V.39/418, ZPAL V.39/419 and numerous more or less fragmentary costals). This allows partial reconstruction of the suture layout. The composition of the shell in *Prot. porebensis* is expected to be mostly the same as that of *Prot. robusta*, and this is supported by the gathered material with small (probably specific) differences explained below.

Noteworthy is a significant variation in thickness and degree of ankylosis of turtle remains found in Poręba. There is no obvious pattern of correlation between the size of the specimen and presence or loss of sutures. Some small specimens appear to have their shells fully fused, and yet there are numerous instances of costals and other elements of subadult or adult dimensions isolated along non-obliterated sutures. There is, however, no morphological evidence that would support the presence of a second turtle species in Poręba which might have attained sexual maturity (and thus start to ankylose) at smaller body size. Some intraspecific heterochrony in degree of ossification is thus apparent. It is conceivable that these differences were due to sexual dimorphism, but preliminary studies on dimorphism and ontogeny in *Proterochersis* spp. (Szczygielski & Słowiak 2018) suggest there seems to be a full spectrum of sizes in which the ankylosed specimens are found, and size differences between two sexes are insufficient to fully explain ankylosis in the smallest individuals. Overall, it seems that the taphonomic environment in Poręba favoured complete fragmentation of the skeletons. Only well-ankylosed shells seem to be preserved in their entirety (and even they are usually broken; see Szczygielski & Sulej 2016); most other specimens are fragments that were broken off, and the specimens that preserve sutures are always small and almost always just individual bones. Notably, these disarticulated small bones are usually preserved best, with well-preserved surficial texture, nearly no cracks and usually no broken parts, albeit that some of the sutural surfaces may exhibit more or less pronounced weathering or slight mechanical damage, possibly due to post-mortem transport.

Description

Nuchal bone. ZPAL V.39/22 (Fig. 9; Szczygielski & Sulej 2018*a*, figs S2, S4E, movies S4–S7, models S1–S2) reveals that the bone underlying the cervical scute is short and paired; in this specimen only the left one is present with an obvious medial suture. Due to the position and shape of this bone, we interpret it as a paired nuchal. Another possible interpretation is that the anteriormost peripherals contacted medially and the nuchal was retracted posteriorly, as in the extant *Hydromedusa* spp., but we find this explanation less compelling for several reasons. First of all, in *Hydromedusa* spp. the retraction of the nuchal behind the first pair of peripherals resulted in loss of the nuchal embayment and either loss of the cervical scute or its exclusion from the anterior margin of the carapace (J. Sterli, pers. comm. 2018) and these characters are strikingly different than in proterochersids (which have a very pronounced nuchal embayment and well-developed cervical scute). Furthermore, the element interpreted by us as the nuchal in *Prot. porebensis* generally does not resemble the neighbouring peripherals shape-wise. Finally, the nuchal is evolutionarily derived from the paired cleithra and in at least some modern turtles it develops from paired primordia (see below and the extended discussion in Szczygielski & Sulej 2018*a*); the proterochersids (as the oldest and least derived turtles possessing a nuchal) are the most likely candidates to still have it paired. The plesiomorphic character of a paired nuchal is supported for our scorings by the character mapping tool of TNT (Szczygielski & Sulej 2018*a*, tree 2–4). It must be noted that this results from the fact that we treat the nuchal as a modification of the cleithra, and thus score them paired as a single character state (char. 247 = 0). If scored separately, the paired character of the nuchal would be treated as an autapomorphy of *Proterochersis porebensis* due to a lack of other taxa known to possess a paired nuchal *sensu stricto*. Given the limited sampling

of that character, it is thus still possible that the paired nuchal in proterochersids is secondary and appeared as a result of heterochronic postponement of primordia fusion.

The medial suture of the nuchal is straight; its structure is mostly lamellar, with lamellae directed dorsoventrally in its ventral part, anterodorsally in the anterior part and posterodorsally in the posterior part (Szczygielski & Sulej 2018*a*, fig. S4E). The posterior suture of the nuchal runs mostly along the sulcus between the cervical and the first vertebral scute; it is partly obscured by sediment in dorsal view, but clearly visible in ventral view. Only in the medial part does the sulcus enter the area of the nuchal, so in medial view the bone is comma-shaped. The suture dividing the nuchal and the first peripheral is directed anteroposteriorly in dorsal view and contained in the area of the cervical scute at the level of the mesial limit of the first marginal. Ventrally, this suture is directed posterolaterally and located slightly posteromedially from the sulcus.

Neurals and preneurals. There are two isolated neural bones known for *Proterochersis porebensis*: ZPAL V.39/4 (Fig. 10A–B) and ZPAL V.39/416 (Fig. 10C–D). Both are hexagonal, coffin-shaped. ZPAL V.39/4 is crossed, slightly anterior to its widest place, by an ω-shaped transverse sulcus, while ZPAL V.39/416 is smooth. This indicates that at least two elements in the neural set of *Prot. porebensis* were hexagonal. The sulcus indicates that at least in ZPAL V.39/4, the shorter end was turned cranially. Orientation of ZPAL V.39/416 is currently impossible. The sutures are mostly lamellar, the lamellae spread in a fan-like fashion from the visceral region in the middle part of the neural.

Behind the nuchal of ZPAL V.39/22 (Fig. 9; Szczygielski & Sulej 2018*a*, fig. S2) there is an element that we interpret as a preneural based on a comparison with SMNS 16442 (although it may potentially represent the first neural expanded anteriorly). The preserved part of the lateral suture of that element is straight and directed anteroposteriorly (at the level of the lateral nuchal suture as visible in dorsal view). Other than that, little can be said about its shape.

Costals. Numerous fragments of isolated costals of different sizes and thickness are known from Poręba, among them ZPAL V.39/3 (Fig. 11C, F), ZPAL V.39/11 (Fig. 11G–H), ZPAL V.39/51 (Fig. 11D–E), ZPAL V.39/235 (Fig. 11A–B; Szczygielski & Sulej 2018*a*, fig. S4C) and ZPAL V.39/419 (Fig. 12R–W). The thinnest of them have edges approximately 2 mm thick and have primarily lamellar sutures with lamellae set approximately along the long axis of the costal in its visceral part and curving dorsally closer to the external surface (Szczygielski & Sulej 2018*a*, fig. S4C–D), while the thickest have their edges more than 1 cm thick and in some cases exhibit a coarse, three-dimensional organization of lamellae in sutures of the proximal part (e.g. ZPAL V.39/3). Ventral surfaces are smooth, and in most cases gently bulging along the middle (e.g. ZPAL V.39/3, V.39/235, ZPAL V.39/419) but in some instances a more substantial, rounded ridge runs along a significant part of the costal (e.g. ZPAL V.39/11 and ZPAL V.39/51). As mentioned by Gaffney (1990) and Szczygielski & Sulej (2016), longitudinal grooves on the visceral surfaces of costals (probable vascular or nerve imprints) are located in the proximity of intercostal sutures but are not remnants of the sutures themselves. This is clearly visible in ZPAL V39/235 (Fig. 11B) and ZPAL V.39/419 (Fig. 12S). ZPAL V.39/3 is unusual in possessing an irregular anterior process in its proximal part.

The external surface of the proximal part of ZPAL V.39/51 (Fig. 11D–E), an isolated costal, is slightly elevated and rugose while the distal part is smoother but covered in low longitudinal ridges and groves. This may be compared to ZPAL V.39/20 and ZPAL V.39/419 (Figs 12A–B, R–W, 13; see below); on the other hand the distal part of ZPAL V.39/51 is more reminiscent of the exposed distal ends of ribs sticking out of the costal plates in, for example, modern chelonioids, chelydrids or trionychids, and may result from an incomplete metaplastic ossification of costals caused by a young ontogenetic age of the individual (the costal plate of that specimen is only 2–3 mm thick). Unlike the mentioned water-inhabiting taxa, the smoother distal part of ZPAL V.39/51 is as wide as the rugose part, which indicates a lack of fontanelles, at least in the preserved section.

Carapacial osteodermal mosaic. Just as in *Proterochersis robusta*, there is a mosaic of numerous dermal bones in the nuchal and pygal region of the *Prot. porebensis* carapace. This is evidenced by several specimens.

ZPAL V.39/22 (Fig. 9; Szczygielski & Sulej 2018*a*, fig. S2) reveals the morphology of the nuchal region. The presence of additional elements in the anterior region of the carapace is clearly visible in that specimen. Most of its sutures are unambiguous and visible in both dorsal and ventral view. Their interdigitation, especially in ventral view, is prominent and they remain closed, refuting possible interpretation as breaks (Szczygielski & Sulej 2018*a*, fig. S2). The comparison of the anterior carapacial bone layout of that specimen with SMNS 16442 is very difficult, given the poor state of preservation of the latter, interrupted identifiable sutures and a near lack of overlap between these two specimens (ZPAL V.39/22 consists mostly of the cervical and anterior marginal scute areas, which are entirely missing in SMNS 16442).

There are some apparent cracks lateral to the nuchal bone, at the lateral region of the cervical scute area. They differ from sutures by their poorly developed interdigitation or complete lack thereof. There is an arguable, weakly interdigitating crack directed anterolaterally across the area of the first marginal scute. This may potentially be a suture, but it differs morphologically from the other sutures of that specimen, so this is uncertain. The suture between the first two peripherals is straight dorsally and runs within the sulcus between the first two marginals, while in ventral view it is sinuous and in the basal part located slightly mesial to that sulcus.

Posteroventrally, there is an articulation site which apparently received the anterior limit of the first costal bone. Despite the well-developed sutures visible in that specimen, this articulation site lacks any sutural characteristics; its internal surface is rugose, but lacks any lamellae or spikes typical of a suture. Given the good state of preservation and lack of exposed bone trabeculae indicative of bone damage, it is unlikely that such sutural structures were initially present and subsequently destroyed. This articulation site is embraced anteriorly by posteroventral flanges of peripherals, medioanteriorly by the

posterolateroventral flange of the nuchal bone, and medially by a short ventrolateral flange of preneural. The latter element separates the articulation site from the contralateral half of the shell. Between the nuchal, partially preserved three peripherals, and part of the preneural, and posterior to the ventral flange of the first peripheral, at least four additional ossifications seem to be present (α, β, γ and δ on Fig. 9) that form much of the roof and floor of the articulation site. The presence of the articulation site for the first costal forces the interpretation of these elements as the supernumerary bones, which are not present in modern turtles and lack strict homology with any elements of the shell in modern turtles; the nuchal, (pre)neural and costal bones are the only elements normally occurring in that region. This is also supported by the anteroposterior position of these elements in relation to the first costal (the diagonal suture between the elements β and γ cannot be an intercostal suture, because obviously there are no costals in front of the first costal). At least in that region, the costal was thus covered both dorsally and viscerally by dermal elements. This multi-layered organization is probably the reason why the anterior rim of the carapace, just posterior to the marginals, is so thick in *Proterochersis* spp. In posterior view, the thickness of the majority of the preneural is approximately the same as the thickness of the elements building the roof of the articulation site, but laterally, just by the medial end of the articulation site, the preneural doubles its thickness, thus both attaining its contact with the bones of the articulation site roof and creating a medial wall of the articulation site. The sutures of these supernumerary bones are heavily interdigitated, especially on the ventral surfaces of the specimen, and in most cases easily and unmistakably distinguishable from breaks and cracks. The element α is a trapezoid ossification surrounded by the first, second and the apparent third peripheral, and the sulcus between the second marginal and the first vertebral scute (which contains a suture, best visible in ventral view). The suture dividing both this element and the second peripheral from the third peripheral is located around the middle of the second marginal, slightly sinuous and directed anterolaterally. The element β contacts the first peripheral anteriorly, the element α anterolaterally, the third peripheral laterally, and the element γ posterolaterally. The anterior and anterolateral suture of that element runs along the cervicovertebral and marginovertebral sulcus, while the posterolateral is directed anterolaterally and contained within the area of the first vertebral scute. Only a small fragment of the element γ is preserved; it contacts the element α anteromedially and the third peripheral anterolaterally (suture running along the marginovertebral sulcus). The sutures around the elements β and γ are best visible in ventral view, where they exhibit much more profound interdigitation than in dorsal view. The element δ is another small, triangular bone located ventrally, behind the suture dividing the first two peripherals, and divided from the first peripheral by a weakly digitated suture. This part was potentially prone to breakage, but observation of the fine detail of this contact confirms the sutural character of this connection. In the lateral part of the specimen there is a roughly rectangular bone fragment, which we parsimoniously interpret as the third peripheral, although given the presence of the element α at the base of the second peripheral, this interpretation is not unambiguous. See Szczygielski & Sulej (2018*a*, movies S4–S7, models S1–S2) for CT scans of this specimen.

A similar articulation site, but with only one flange (either dorsal or ventral) is present in the partial peripheral ZPAL V.39/55 (Fig. 15A–C), but it is unknown whether this specimen comes from the anterior or posterior part of the carapace. The tip of this peripheral is gently curled away from the articulation site, but this is of little use because the tips of peripherals are curled ventrally in the anterior region of the carapace, but dorsally in the posterior region.

ZPAL V.39/20 (Figs 12A–B, 13) is a set of proximal parts of two articulated costals, most probably the eighth and ninth based on their shape and size. Their external surface has two distinct textures (Figs 12A, 13E, G–L): in the proximal part, there is an ovoid, gently elevated patch of rugose vascular ornamentation, typical for *Proterochersis* spp. Distally, however, the surface is slightly depressed, wavy and perforated by numerous vascular foramina, but the external cortex is smooth and shiny. This does not seem to be a result of imperfect ossification, because the costals are thick (0.5–1.1 cm) and possess a well-developed external cortex even in the distal region (Fig. 13A–D). This area belongs to the posterior part of the carapace and corresponds to the mosaic-covered section of SMNS 17755a. It is thus possible that the wavy area, which apparently was removed from the overlying epidermal scutes, was covered by numerous, more external ossifications, just like in SMNS 17755a. The wavy but shiny external surface of the distal region of ZPAL V.39/20 is reminiscent of the surface of ribs in *Pappochelys rosinae* (SMNS 91360, SMNS 91895; see also Schoch & Sues 2015, 2018) especially in the posterior part. In the posterior part, this area shows more lamellar, suture-like relief, and possibly it accommodated the sutural edges of the osteodermal platelets forming the mosaic.

A similar morphology is presented by ZPAL V.39/419 (Fig. 12R–W), a single, incomplete, isolated costal. This specimen is thinner (4–6 mm) than ZPAL V.39/20, and on its external surface it bears a straight, longitudinal sulcus, which may be identified with confidence as an intervertebral sulcus (Fig. 12R, T). Similar to ZPAL V.39/20, in its distal part the costal presents a depressed area which lacks typical, rough texture (Fig. 12R, T–W). Only minor sections of the depressed surface are preserved in that specimen, but they exhibit longitudinal striation (Fig. 12T–U) intermediate between the suture-like relief seen in the posterior part of ZPAL V.39/20 and the gently striated distal part of ZPAL V.39/51. The walls of the depressed area have an irregular course and they have a coarser, suture-like texture, very similar to the intercostal sutures preserved on the edges of that specimen, which in this part become reticulate rather than lamellar (Fig. 12T–W; Szczygielski & Sulej 2018*a*, fig. S4D, G). On the anterior, undamaged edge, it is evident that the intercostal suture and the depression wall are continuous with one another (Fig. 12V) and that in the proximal part of the specimen the costal is a single element throughout its depth. In the preserved section neither the walls nor the floor of the depression show any sign of damage.

Several isolated, polygonal bony platelets of varied thickness, usually with radial vascularization pattern, were found in Poręba, of which ZPAL V.39/373 (Fig. 12E–F), ZPAL V.39/374

(Fig. 12G–H) and ZPAL V.39/375 (Fig. 12C–D) are complete, have sutural edges all around, and present at least some of the unmistakable turtle characteristics: rough texture with imprints of dermal vasculature, wavy sulci and eccentric tubercles reminiscent of those present near the dorsoposterior edge of the pleural scutes. They may represent the superficial ossifications visible in SMNS 17755a. The identification of ZPAL V.39/373 as coming from the dorsoposterior pleural scute region is supported both by the sulci layout (along the dorsal and dorsoposterior edge of the platelet) and the shape and location of the boss. The radial organization of the vasculature and fine details of the visceral surface are particularly prominent in this specimen, supporting its identity as a separate dermal ossification, and not part of a costal bone. Another very similar, boss-bearing but uncomplete specimen, ZPAV V.39/417, was also found; the preserved section exhibits no sulci, but is otherwise very similar to ZPAL V.39/373. Part of that specimen is missing, making confirmation of all the sutural edges impossible, but the sutures are certainly present along the edges identifiable, based on the position and shape of the boss, as dorsomedial (i.e. towards the pleurovertebral sulcus) and ventrolateral (i.e. towards the pleuro (supra)marginal sulcus) edges, refuting the identity of that element as a part of a costal. ZPAL V.39/374 also bears a tubercle-like structure on its external surface, and therefore may come from a comparable area of the shell, but the shape of the tubercle is less typical (it is more angular, which may be caused by the larger size of that specimen; ZPAL V.39/374 is the thickest of the three with an edge up to 1.1 cm thick) so this interpretation is uncertain. ZPAL V.39/375 lacks features that would allow its positioning in the shell but exhibits generally the same surficial characteristics and a shallow, straight groove, which we interpret as a poorly defined sulcus. Similar straight sulci occur in some regions of the proterochersid carapace, for example, between the vertebral scutes, between the marginals, and between the supramarginals (Szczygielski & Sulej 2016). ZPAL V.39/375 is the thinnest and smallest ossicle (edge 2–4 mm thick) and has a serrated (spiky) sutural edge, while the ZPAL V.39/374 has complex, partly spiky and partly lamellar sutural edges. It must be noted that the posterior section of the carapace in *Proterochersis* spp. does not rapidly decrease its thickness in comparison to other regions (although, at least in ZPAL V.39/48, the carapace is very thin along the anterior sulcus of the fifth vertebral scute, in places no more than 2–3 mm thick), so more posterior ossifications are expected to be thicker than the ones overlying the ribs, and to lie in the same plane as costals and neurals. This is affirmed by ZPAL V.39/167 (Fig. 12K–Q), a posterior left peripheral with at least four additional, irregular ossifications attached. These ossifications vary in size but all are relatively thick (up to 1 cm) and, as in ZPAL V.39/374, their sutures are complex, partly spiky and partly lamellar. The peripheral itself is normal, approximately rectangular, with the upper suture located slightly below the pleuromarginal sulcus. The same shape is also present in comparable (but coming from the left side of the shell) peripheral ZPAL V.39/181 (Fig. 15L–O). This element lacks any additional ossifications and is V-shaped in anterior, and triangular in posterior view. Its tip is gently bent towards the outer surface. The sutures of posterior peripherals are the same as in bridge peripherals. ZPAL V.39/418 (Fig. 12I–J) is another irregular, small ossicle with complex sutural edges (Szczygielski & Sulej 2018*a*, fig. S4F) and an undulating sulcus, but it differs from the aforementioned bony plates in its heavily vascularized, rough surface on both sides rather than only on one (external) side. The details of the texture slightly differ between the sides: the sulcus-bearing surface is more coarsely textured and perforated by more numerous vascular openings than the other surface. The latter, however, still differs from typical, smooth visceral surfaces of the remaining isolated bony plates, costals or neurals and is more reminiscent of the scute-covered exterior of the carapace. Therefore, it seems likely that ZPAL V.39/418 comes from the shell margin and was covered by marginal scutes from both sides.

The identification of ZPAL V.39/22 and ZPAL V.39/167 as turtle remains is uncontroversial; both exhibit typical, turtle-like surficial texture and a sulcus layout congruent with that of *Proterochersis porebensis*, which allows their precise allocation in the shell. Likewise, the scutes and underlying osteoderms lack one-to-one numerical correspondence. ZPAL V.39/20 lacks visible sulci, but comprises two costal bones sutured together with a visible suture between them, preserves anterior sutural surface with preceding costal, and broken but recognizable remains of rib necks. Broad, sutured together ribs are diagnostic only for true turtles (Testudinata) and *Prot. porebensis* is the only Triassic turtle known from Poland, hence this specimen is identified as such. Finally, ZPAL V.39/419 is also an obvious turtle costal with sutural edges and a sulcus identifiable as an intervertebral sculcus. The remaining specimens (ZPAL V.39/373, ZPAL V.39/374, ZPAL V.39/375) are isolated bony platelets, so their interpretation is more difficult, but all of them exhibit the same surficial characteristics and have sulci (undulating in the case of ZPAL V.39/373, ZPAL V.39/374 and ZPAL V.39/418) which support their identification as parts of the turtle shell. ZPAL V.39/373 and ZPAL V.39/417 additionally bear an asymmetrical boss, so they can be readily identified as posterodorsal parts of a pleural scute. See Discussion for comparisons with other taxa.

Pygal region of the carapace. There are three specimens of the posteriormost peripheral that show sutural layout: ZPAL V.39/23 (Fig. 14A–B) and ZPAL V.39/213 (Fig. 14E–F), both coming from the left side of the carapace, and ZPAL V.39/54 (Fig. 14C–D) from the right side. ZPAL V.39/23 (Fig. 14A–B) bears the complete last and part of the preceding marginal and a fragment of the last vertebral scute. It apparently belonged to a small specimen; the last marginal is maximally 1.9 cm long, with 1 or 2 mm missing from its distal tip. The suture with the preceding peripheral is diagonal, directed posterolaterally and lamellar, with deep grooves between the lamellae in the area of the second-to-last marginal scute, and much less pronounced lamellae in the area of the last vertebral scute. The medial end of the specimen is broken, so only a small part of the natural edge of the caudal notch is preserved. Ventrally, there is a smooth-surfaced fossa or embayment present, which apparently accommodated the posterior process of the ilium. ZPAL V.39/213 (Fig. 14E–F) is much larger (maximally 4.2 cm long) and consists of the area of the last marginal and a small fragment of the last vertebral scute. The second-to-last peripheral is not

preserved; only a small amount of bone tissue with no natural surface is present mesial to the interperipheral sulcus. There is a suture visible crossing the anteriormost part of the last marginal area and the posterolateral corner of the last vertebral scute area. This differs slightly from ZPAL V.39/23, in which the suture never enters the area of the last peripheral and goes deeper onto the area of the last vertebral scute. This difference may be attributed to either the ontogenetic age of the specimen or interspecific variation. The layout of the bony mosaic seen in SMNS 17755a is highly irregular, so it is possible that the sutures surrounding the posterior peripherals were also more or less irregular. Another possibility is that the difference results from the number of marginals and peripherals present in given animal; in *Proterochersis porebensis* variants with 14 or 15 marginal scutes are known, and the number of peripherals probably impacted the layout of sutures in relation to the overlying scutes. ZPAL V.39/54 (Fig. 14C–D) is intermediate in size (2.5 cm long, as preserved) and shows approximately the same morphology and suture layout as ZPAL V.39/213, but its sutural surfaces are poorly preserved.

Szczygielski & Sulej (2016) reported that at least the first sacral vertebra of *Proterochersis porebensis* was connected to the shell. This morphology is confirmed by a newly found specimen, ZPAL V.39/402 (Fig. 14G–J), in which an osseous connection between both sacral vertebrae can be clearly seen. Due to suture-obscuring ankylosis, the exact character of that contact (whether the sacrals form their own neurals or if they are only attached to the visceral surface of overlying dermal bones) remains uncertain. This specimen is a part of a large individual, comparable in size to ZPAL V.39/49 (carapace length approximately 50 cm), so it is also unclear whether both sacrals were connected to the carapace in younger animals. Only a small middle section of the caudal notch edge is preserved in ZPAL V.39/402, but its curvature is virtually the same as in ZPAL V.39/49, so the notch may be safely estimated to be triangular, consistent with other *Prot. porebensis* specimens but different to that of *Prot. robusta*.

The broken anteromedial edge of ZPAL V.39/59 (fragment of the posterior left part of the carapace) reveals that the posterior process of ilium (as interpreted by Szczygielski & Sulej 2016) is separated from the overlying carapace by a band of compact bone (presumably cortices of both elements). This is congruent with the interpretation of that structure as a homologue of posterior ilial process of other Triassic turtles and thus, as part of the pelvis (contra Joyce *et al*. 2013). Other than that, this specimen exhibits no sutures.

Bridge. The bridge regions of *Proterochersis porebensis* are usually broken or not preserved, but there are several specimens of isolated peripherals from that area (most notably ZPAL V.39/14, ZPAL V.39/21 and ZPAL V.39/173; Fig. 15D–K; Szczygielski & Sulej 2018*a*, fig S4H), with at least some of their sutural surfaces intact. Generally, as in *Prot. robusta* and most other turtles, the interperipheral sutures do not coincide with the intermarginal sulci but are located in the posterior parts of the marginals (this is also true for most other peripherals, as shown by ZPAL V.39/55, ZPAL V.39/167 and ZPAL V.39/181; but not all of them: see ZPAL V.39/22). Unlike *Prot. robusta*, in *Prot. porebensis* the costoperipheral sutures are located not near the midline of the supramarginals, but rather below them, around the dorsal sulci of marginals. The costoperipheral sutures show a complex arrangement of lamellae; the interperipheral sutures usually are lamellar, with lamellae radiating from the middle of the element, or spiky, with denticle-like processes running towards the neighbouring element.

In several specimens (ZPAL V.39/5, ZPAL V.39/8, ZPAL V.39/48, ZPAL V.39/49, ZPAL V.39/376; Fig. 16A, D–H, L, M) along the visceral surface of the bridge region there are bands of cancellous bone with intertrabecular spaces filled with rock matrix. In ZPAL V.39/5 and V.39/376 such a band is present dorsally, but towards the middle part of the specimen the cancellous bone grades into the matrix. This matrix is partially removed in the ventral part of the specimen, exposing an empty trough lined with bone cortex (no cancellous bone exposed). A similar trough is also present in ZPAL V.39/168. The shape and size of that trough corresponds with the protruding apical ends of the dorsal ribs in the bridge of *Prot. robusta* (mainly SMNS 12777, Fig. 16N, and CSMM specimen) described above. The sutures are not visible in any of the specimens with the cancellous band and trough preserved but, taking into account the position of costoperipheral sutures in ZPAL V.39/14 and ZPAL V.39/173, the cancellous band and at least the dorsal part of the trough were restricted to costals and did not enter the area of the peripherals. The exposed cancellous bone and its gradual disappearance in ZPAL V.39/5 may indicate that these rib apices were not yet fully ossified and were at least partially cartilaginous. We exclude the possibility of erosion or decomposition of these apical parts, because the surrounding bone is not eroded and does not show any particular signs of pre-burial decomposition. Additionally, the presence of troughs in the visceral surfaces of peripherals proves that these distal parts of ribs were in life separate from the bone tissue of the peripherals. The cancellous bands are relatively smooth, making it unlikely that the substantia spongiosa was exposed as an effect of a break, and the intertrabecular spaces are filled with the same mudstone as the one surrounding the specimens, rather than mineral crystals, which indicates that they were in contact with the environment early during diagenesis. In ZPAL V.39/21 (Fig. 16I–K) there is a round canal penetrating the peripheral dorsally, just lateral to the preserved part of the costoperipheral suture. This canal may potentially represent a bite mark, but it is comparable in diameter (7 mm) with the troughs visible in ZPAL V.39/5 (6–8 mm) and ZPAL V.39/168 (8 mm), so it may be an entrance point of the rib apex. On the visceral surface of ZPAL V.39/21 (Fig. 16I) the peripheral is covered by what looks like a bony sheath, which in most part appears to be separate, but in the dorsal part joins the peripheral seamlessly. Possibly, at some stage of development, the rib apices were therefore covered viscerally by the peripherals, or there was some variation in relative positions of these elements. In ZPAL V.39/8 (Fig. 16A), besides two bands of exposed cancellous bone, one ossified rib end is seen protruding, but this is probably the apex of the first costal (the second dorsal rib). In the anterior region of the carapace, the troughs or bands of cancellous bone are tilted posteroventrally in relation to the axis of the peripherals, partly due to anterodorsal inclination of the anterior carapacial rim.

Epiplastra. The epiplastra of *Proterochersis porebensis* supported the lateral part of the gular scutes (the medial parts were overlying the entoplastra, as evidenced by SMNS 16442) and medial parts of the extragular scutes, as evidenced by ZPAL V.39/404 (Fig. 17), a disarticulated epiplastron. This specimen is complete with the exception of the dorsal process, which was broken off at its base. The morphology and position of the sutural area generally corresponds with the morphology of the entoplastron of SMNS 16442. There is a suture laterally, which must have received another ossification supporting the lateral part of the extragular scute. This might have been either an anterior expansion of the hyoplastron reaching the anterior edge of the plastron, or a supernumerary bone. The former would imply a significantly different shape of the hyoplastron from that observed in *Proterochersis robusta* specimen SMNS 16442, in which the hyoplastron stretches no further than to the humeroextragular scute, whereas the latter seems to be supported by ZPAL V.39/186 (see below). The sutures mostly have a lamellar structure. The initial position of clavicles deep to the other plastral elements is developmentally recapitulated in modern turtles; the clavicular primordia originate above the plastral mesenchyme, which they enter later during embryogenesis (Vallén 1942; Walker 1947; Cherepanov 1989).

Extragular ossification. ZPAL V.39/186 (Fig. 17M–T) represents a lateral part of the extragular tubercle, as evidenced by its shape and bowed sulcus on its dorsoposterior surface. This element seems to preserve partially damaged sutural edges. Medially, there is a probable suture for the epiplastron, best preserved in the anterior part of the element (Fig. 17R). This suture is slightly skewed anterolaterally and exhibits longitudinal lamellar organization; both characteristics corresponding to the lateral suture of ZPAL V.39/404. Posteriorly (Fig. 17P, S–T), the element has rounded, unbroken edges (Fig. 17P, T). In its lateral part a suture-like lamellae are partially exposed from the sediment (Fig. 17P) and more medially a field of undamaged cortical bone (Fig. 17T) is present. These features are significantly different from the spongy internal structure of damaged bone, visible in the medioposterior section of the specimen (Fig. 17R). The shape and contacts of ZPAL V.39/186 fit the morphologies seen in SMNS 16442 (ento- and hyoplastra of *Proterochersis robusta*) and ZPAL V.39/404 (epiplastron of *Prot. porebensis*) and suggest that the former was separate from both the epiplastron and the hyoplastron, and thus is an additional ossification not homologous to any plastral bones of derived turtles. Unfortunately, the state of preservation of the medial sutural surface of that specimen is subpar, their surfaces in many places are slightly abraded, and the details of the posterior suture are obscured by hard matrix, so further preparation is likely to result in more damage. Therefore, our interpretation of that small element should be taken with caution.

Xiphiplastra and supernumerary posterior plastral elements. ZPAL V.39/170 (Fig. 18I) is an isolated left xiphiplastron, as evidenced by its shape and diagonal femoroanal sulcus crossing its external surface, and presents sutural contacts of the xiphiplastron. The visceral surface is badly damaged and presents no discernible characters, save from the low elevation in the place where the lateral pubic process was attached. Its medial edge contacted the contralateral xiphiplastron, the anterior edge was attached to the hyoplastron, but the posterior, Z-shaped (in visceral view) suture has no counterpart with other turtles. In the same area, faint sutures may be observed also in ZPAL V.39/13 (Fig. 18A–C), ZPAL V.39/68 (Fig. 18G) and ZPAL V.39/69 (Fig. 18D–F), although these sutures lack a lateral embayment as deep as the one present in ZPAL V.39/170, and are positioned more similarly to the analogous suture in SMNS 16442 (Fig. 8D). The sutures can be also seen between the posterior processes and the medial part, approximately in the same manner, as the sulci delimitating the intercaudal scute from the caudal scutes. The pattern of vascularization visible in ZPAL V.39/13 and ZPAL V.39/69 also suggests that this region is built from three separate ossifications, here termed supernumerary posterior plastral elements (SPPEs). In no specimen of either *Proterochersis porebensis* or *Prot. robusta* is the medial element divided in half by a medial suture, as would be expected if it was a part of the xiphiplastron; only in ZPAL V.39/13 it is split, but that specimen is clearly broken longitudinally in three places, not only along the midline, but also in two places along the right xiphiplastron. Other than that, the median element is always either completely missing, or completely present. The lack of medial suture dividing the medial element is especially well exhibited by ZPAL V.39/68 (Fig. 18G), in which the median suture dividing both xiphiplastra splits in two and runs along the sulci of intercaudal scute. There is some disparity in *Proterochersis* spp. when it comes to the position of sutures dividing the SPPEs (e.g. in ZPAL V.39/170 the lateral parts of the suture are positioned more cranially than the medial part, while in ZPAL V.39/13, ZPAL V.39/69 and SMNS 16442 these relations are switched; both in ZPAL V.39/170 and SMNS 16442 the suture is confined to the area of the anal scutes, while in ZPAL V.39/13 and ZPAL V.39/69 they seem to follow the sulci around the intercaudal and caudal scutes; see Figs 8 and 18). Although this may also suggest that there was another ossification present that filled the lateral embayment visible in ZPAL V.39/170 and contacted the base of the posterior processes, there is currently no evidence that would support this, and the variation may be more parsimoniously attributed to the intraspecific, sexual or even ontogenetic variation (especially that there is an obvious variation in the size and shape of said scutes). There are some more or less symmetrical breaks around that region in the holotypes of *Prot. robusta* (SMNS 12777: along the sulci between both anal scutes, caudal scutes, and intercaudal scute) and *Prot. porebensis* (ZPAL V.39/48: near the base of posterior processes), as well as in *Prot. porebensis* specimen ZPAL V.39/49 (near the base of posterior processes) that might potentially follow the layout of sutures, but this is ambiguous.

PHYLOGENETIC ANALYSIS

*Analysis 1 (*C. tenertesta *scoring variant A)*

When *Chinlechelys tenertesta* was scored as having cervical osteoderms (char. 251 = 1) but with the presence of the mosaic scored as unknown (char. 249 = ?), the analysis

yielded 12 400 trees (best score 1007, hit 140 times, CI 0.317, RI 0.766). The resulting strict consensus tree (Szczygielski & Sulej 2018*a*, tree 1) is poorly resolved, and most stem Testudinata, including *Proterochersis* spp. and *C. tenertesta* are gathered in a large polytomy.

*Analysis 2 (*C. tenertesta *scoring variant B)*

When *Chinlechelys tenertesta* was scored as having both the cervical osteoderms (char. 251 = 1) and the osteodermal mosaic within the shell (char. 249 = 0), the analysis yielded 10 100 trees (best score 1007, hit 158 times, CI 0.317, RI 0.766). The resulting strict consensus tree (Szczygielski & Sulej 2018*a*, tree 2) is better resolved, and *C. tenertesta* is recovered in a weakly supported (Jackknife value 15) polytomy together with *Proterochersis robusta* and *Prot. porebensis* at the base of Testudinata, as a sister group to *Proganochelys quenstedti* and all more derived turtles. The clade shares two common synapomorphies in all trees: character 229 0 → 1 (costo-peripheral fontanelles absent, distal end of posterior dorsal ribs visible or distal end of posterior costals narrow and surrounded by the peripheral) and character 249 1 → 0 (carapacial mosaic present). The mosaic is thus optimized as a synapomorphy of this clade.

*Analysis 3 (*C. tenertesta *scoring variant C)*

When *Chinlechelys tenertesta* was scored as having no cervical osteoderms (char. 251 = 0) but having the osteodermal mosaic within the shell (char. 249 = 0), the analysis yielded 10 600 trees (best score 1006, hit 165 times, CI 0.317, RI 0.767). The resulting strict consensus tree (Fig. 19; Szczygielski & Sulej 2018*a*, tree 3) is topologically the same as the tree obtained in the analysis 2, but the polytomy between *Proterochersis* spp. and *C. tenertesta* is resolved. The Jackknife support is 57 for the *Proterochersis* spp. clade exclusive of *C. tenertesta*, and 19 for the *Proterochersis* spp. + *C. tenertesta* clade. The common synapomorphies for the latter are the same as in the analysis 2 (char. 229 = 1, char. 249 = 0).

Analysis 4 (no C. tenertesta*)*

When no *C. tenertesta* scoring variant was used, the analysis yielded 12 100 trees (best score 1005, hit 170 times, CI 0.317, RI 0.767). The resulting strict consensus tree (Szczygielski & Sulej 2018*a*, tree 4) is the same as in the analyses 2 and 3, but the support values for the testudinate stem are higher, especially for Proterochersidae (Jackknife value 87) and for the clade of *Proganochelys quenstedti* and more derived turtles (81), strongly supporting the position of Proterochersidae at the base of Testudinata, as previously demonstrated by Szczygielski & Sulej (2016). The *Proganochelys*–testudinate clade exclusive of Proterochersidae is supported in all trees by five common synapomorphies: character 244 (number of abdominal scutes) 0 → 1 (one pair), character 245 (number of dorsal vertebrae) 0 → 1 (10 + one intermediate cervicodorsal), character 248 (coracoid shape) 0 → 1 (flat, rectangular), character 254 (posterior notch in hypoplastron) 1 → 0 (present, one or more notches receive anterior processes of xiphiplastron) and character 255 (shape of the articular surface of femoral head in dorsal view) 1 → 2 (articular surface rectangular or oval in dorsal view).

The topology presented here differs from the preliminary topologies reported by Szczygielski & Sulej (2018*b*), based on Jacknife trees produced from a smaller version of the matrix used herein, in which *C. tenertesta* was recovered separate from *Proterochersis* spp. and crownward to *Prog. quenstedti*.

DISCUSSION

Taxonomic identification

Several specimens described herein are built from numerous supernumerary bones that are unknown in modern turtles and thus, based on composition alone, would not be normally identified as testudinates. Their identification as turtles is, however, unambiguous. Besides their origin from the same localities, in which complete shells of *Proterochersis* were found (Murrhardt and Poręba), they exhibit several unmistakably chelonian characteristics. Their size, thickness and surficial characteristics are comparable with other specimens of *Proterochersis* coming from the same localities. The most diagnostic is, however, the presence, morphology and organization of the scute sulci.

SMNS 17755a (Fig. 2; Szczygielski & Sulej 2018*a*, fig. S1A–C) preserves sulci delineating three rows of large, polygonal scutes that are identical to vertebral, pleural and marginal scutes in a manner exclusive for turtles. This excludes this specimen from any other armoured Triassic reptile taxon, because most of them (e.g. aetosaurs, phytosaurs, rauisuchians) completely lack sulci on their dermal ossifications (Scheyer & Sander 2007; Scheyer & Desojo 2011; Scheyer *et al.* 2014). Furthermore, SMNS 17755a differs from most archosauromorphs in its lack of pitted or grooved ornamentation and in its randomized layout and shape of elements. The only taxon that preserves sulci on dermal armour and which can be compared in terms of general morphology and layout of ossifications (see below) is Cyamodontoidea.

Cyamodontoid placodonts, however, typically exhibit an approximate one-to-one correspondence in number of osteoderms and scutes; their scutes are small, numerous, and frequently more symmetrical (Westphal 1975; Rieppel 2002). Additionally, they inhabited marine environments, so their appearance in alluvial sediments of the Löwenstein Formation (Hornung & Aigner 1999) would be surprising. The shape, relative size and relative positions of these scutes are identical to those of other *Proterochersis* spp. specimens (cf. Szczygielski & Sulej 2016 and Szczygielski & Sulej 2018*a*, fig. S3A, C). Most of the sulci are gently undulating (Fig. 2) and there is an eccentric and asymmetrical boss or tubercle located in the posterodorsal section of each pleural scute area, which is characteristic of Late Triassic turtles (Gaffney 1985, 1990; Szczygielski & Sulej 2016). There is no ridge running along the preserved posterior edge of the fourth vertebral scute, so this specimen cannot be identified as *Keuperotesta limendorsa*. There is no supramarginal row of scutes, so the specimen does not belong to the only remaining Norian turtle known from Germany, *Proganochelys quenstedti*. Furthermore, the CT scans (Szczygielski & Sulej 2018*a*, movies S1–3) reveal outlines of the sacrum and both ilia, which had an osseous contact with the carapace in *Proterochersis* spp., but not in *Prog. quenstedti* (see Gaffney 1990; Szczygielski & Sulej 2016) or any non-testudinate reptile. The identification as *Proterochersis robusta* is therefore clear.

Is the mosaic a proterochersid autapomorphy?

A carapacial osteodermal mosaic, similarly to that in proterochersids, is present in another, North American Norian turtle, *Chinlechelys tenertesta*. The complex spikes of that turtle are usually interpreted as cervical osteoderms (after Joyce *et al.* 2009), but were also initially proposed to be a part of the posterior margin of carapace (Lucas *et al.* 2000). In any case, they represent an osteodermal mosaic in roughly the same region as that observed by us in *Proterochersis* spp. Furthermore, some additional data supporting the presence of the mosaic in the non-marginal part of the carapace of *C. tenertesta* were also reported, but not described in detail, by Lichtig & Lucas (2015, 2016). According to our phylogenetic analyses (analysis 2 and 3, see above), this turtle is the sister taxon to *Proterochersis* spp. (Fig. 19; see also Szczygielski & Sulej 2018*a*). This seems to refute the synonymy of genera *Chinlechelys* and *Proganochelys* proposed recently by Joyce (2017) and suggests the affinity of *C. tenertesta* with Proterochersidae. Due to several differences and severe incompleteness of that turtle, it is currently difficult to unambiguously evaluate whether *C. tenertesta* and *Proterochersis* spp. were indeed parts of the same lineage. Besides the similarity of complex dermal spikes of *C. tenertesta* to cervical osteoderms or posterior carapacial rim (see below) of *Prog. quenstedti*, the distinctiveness of *C. tenertesta* from *Proterochersis* spp. is also suggested by a notch in the posterior edge of hypoplastron, which received the anterolateral process of xiphiplastron and is missing in *Proterochersis* spp. and *Odontochelys semitestacea* (Fig. 19). Lichtig & Lucas (2016) argued that *C. tenertesta* branched out from the turtle stem even earlier than *Odontochelys semitestacea*, but the currently known material of this turtle is too fragmentary to support such an assumption, and the intervertebral articulation of ribs of *C. tenertesta* is more advanced than the mid-central articulation of *O. semitestacea*, so unless some new material is published, this remains speculative.

Based on the topologies recovered by us (analyses 2 and 3), given the limited sampling of Triassic taxa, the osteodermal mosaic observed in Proterochersidae and *Chinlechelys tenertesta* is probably a synapomorphy of that clade and appeared either independently or as a result of proliferation of less numerous dermal ossifications present in the common ancestor of proterochersids and more derived turtles. It must be stressed that the composition (number and layout) of the fully dermal parts of the carapace, including the presence of the carapacial osteodermal mosaic, is completely unknown for *Proganochelys quenstedti*, *Palaeochersis talampayensis* or any other Triassic turtle (Gaffney 1990; Sterli *et al.* 2007). Future observations on other, non-proterochersid line, turtles may therefore either confirm this assumption or possibly prove it to be a transitional morphology which led to the development of the typical turtle formula of peripherals, pygal and suprapygal(s) by reduction of the number and ordering of the layout of the mosaic elements. Indirect evidence is, thus far, provided by *Prog. quenstedti*. This turtle has a set of fontanelles in the posterior part of the shell, formed between the distal parts of costals and the peripherals (Gaffney 1990). However, unlike in modern and other fossil turtles, these fontanelles do not penetrate the carapace but are shielded dorsally by bone (Gaffney 1990). This suggests that they were overlain by additional dermal components, as in *Proterochersis* spp., but this remains speculative due to a lack of data on sutures in that region. Additionally, in the Middle Jurassic *Eileanchelys waldmani* Anquetin *et al.* 2009 as well as in numerous Late Jurassic plesiochelyids, thalassemydids and eurysternids, there is an additional, 'intermediate' ossification of varied shape and size located between the eighth neural, the last pair of costals and the first suprapygal (Joyce 2000; Anquetin *et al.* 2009, 2014; Joyce *et al.* 2009; Anquetin & Joyce 2014). The nature of this bone is uncertain, but it may support the view that the pygal region of the carapace was initially composed of a larger number of elements. However, more data is needed to properly interpret the evolution of the dermal carapacial elements.

Anomaly versus the norm

The shell anomalies in turtles are frequent, but they mostly affect the epidermal scutes. Additional bony elements may occur, but they are relatively rarer (Zangerl 1969), although in some taxa or populations they may be present even in 60–70% of specimens (McEwan 1982). Most common among them are additional elements in the posterior region of the carapace (Zangerl 1969; McEwan 1982; Kordikova 2002; Cherepanov 2016; Mautner *et al.* 2017). However, they usually appear as individual, asymmetrical elements and never seem to arise in abundance within one specimen comparable to that seen in *Proterochersis* spp. The randomness of the anomalies also makes it rather unlikely that we will find the same anomaly in two or more specimens, especially with so extremely small sample size as these available for the Triassic turtles. This makes the interpretation of the additional bones observed in *Prot. robusta*, *Prot. porebensis* and *Chinlechelys tenertesta* (regardless of them being a part of the carapace or osteoderms) as mere anomalies unlikely. We also find it unlikely that this unusual composition is a result of some pathology, at least we were not able to identify any disease or malformation with similar effect. Additionally, the congruent morphologies are present in several specimens both from Germany (SMNS 17755a) and Poland (ZPAL V.39/20, ZPAL V.39/167) and is supplemented by isolated ossifications found in Poręba (ZPAL V.39/373, ZPAL V.39/374, ZPAL V.39/375, ZPAL V.39/417, ZPAL V.39/418). Subtle differences in fine surface ornamentation, as well as variance in preservation and colour, indicate that these specimens do not come from a single individual within each locality but rather are parts of several animals.

Some small bony flakes overlying the shell were described by Hay (1922, 1929) from several specimens of matamata, but these platelets differ from the ones observed in *Proterochersis* spp. in a number of aspects: (1) they usually have straight edges; (2) they usually do not appear in groups in one region of the shell; (3) they seem to never form sutural connections with each other and with typical shell elements; (4) they never disturb normal connections between the shell bones.

Even if the observed characters do not represent the norm for *Prot. robusta*, *Prot. porebensis* and *Chinlechelys tenertesta*, they would at least prove that vastly less strict and reliable morphogenesis control mechanisms were present early in the turtle lineage. The relatively large instability of bone layout in the posterior region of carapace in modern turtles was explained as a result of developmental complications related to the presence of the underlying sacral region of the axial skeleton (Zangerl & Johnson 1957), its independence of the axial skeleton (Zangerl 1969) or the lack or low number of arranged invaginations of dermis forming between the epidermal scutes, which appear to regionally promote the osteogenesis (Cherepanov 1989, 2016). While any or all of these causes may be true, the less strict developmental program of the fully dermal part of the carapace may also be related to the phylogenetic ancestry of turtles. Sadly, very little is known about the morphogenetic regulation of the pygal and suprapygal region in turtles and the determination of osteoderm layout in other taxa.

Comparative anatomy of the carapacial osteodermal mosaic

The mosaic of ossifications at the posterior end of the carapace in *Proterochersis* spp. is unexpected. Thus far, it has been assumed that this region was composed in the same manner in Triassic turtles as in more derived taxa, from posterior costals, peripherals, one or several suprapygals, and potentially one pygal (although the caudal notch of proterochersids and *Palaeochersis talampayensis* might have suggested the absence of the latter) but no actual data supported this view. It is currently unknown whether *Keuperotesta limendorsa* exhibited a similar pattern of posterior carapacial ossifications, but representatives of both genera seem to have similar morphology of the shell, and it may therefore be speculated that they did not differ in that aspect either.

The presence of such numerous ossifications in the turtle carapace makes the status of *Priscochelys hegnabrunnensis* from the lower Ladinian of Hegnabrunn worth considering again. This taxon was proposed to be a posterior section of carapace belonging to a stem turtle, as suggested by the presence of turtle-like sulci outlining the epidermal scutes (Karl 2005; Joyce & Karl 2006) but Scheyer (2008) refuted this affinity based on the histological merits (lack of diploe structure, radial vascularization), different surficial texture, and presence of numerous sutures encircling the several separate ossifications that built this specimen. Nonetheless, if the plate corresponds to the external layer of ossifications, and not the costals or peripherals, these differences may not be pivotal. Additionally, the internal surface of the articulation site formed by dermal bones in ZPAL V.39/22 is coarse and quite similar to the visceral surface of the *Pri. hegnabrunnensis* holotype. Still, the texture of the external surface of that specimen is unlike that of turtles, but this may be in part the result of erosion or diagenesis, and partially of the long time separating these taxa; *Pri. hegnabrunnensis* is approximately 5–10 million years older than *Odontochelys semitestacea* and almost 20 million years older than the oldest Testudinata. The ornamentation of the dermal bones evolves relatively fast and differs slightly between the coeval Late Triassic turtle taxa (de Broin 1984) or even within one species (TSz pers. obs. 2018). Additionally, the plastron and costals of early

pantestudinates are relatively smooth (Li *et al.* 2008; Schoch & Sues 2015; TSu 2015 and TSz 2016, pers. obs.) and it is theoretically possible that the surficial ornamentation in the earliest carapace-bearing animals differed from more derived, later forms. In any case, more specimens are needed to resolve this question.

Numerous ossifications forming the carapacial rim of *Proterochersis* spp. may also be compared to the complex spikes of *Chinlechelys tenertesta*, described and figured by Lucas *et al.* (2000) and Joyce *et al.* (2009) as cervical osteoderms similar to those of *Proganochelys quenstedti*. Lucas *et al.* (2000) also briefly noted their similarity to posterior marginal carapace area of the latter, but quickly refuted this possibility due to presence of numerous sutures (Szczygielski & Sulej 2018*a*, fig. S1E). Although the exact configuration of posterior part of the carapace is unknown in *Prog. quenstedti*, the bony mosaic of proterochersids and possible presence of dermal mosaic in other regions of *C. tenertesta* carapace (Lichtig & Lucas 2015, 2016) makes such a comparison viable. The similarity of the structure is prominent (Szczygielski & Sulej 2018*a*, fig. S1). While it is difficult to identify the spikes of *C. tenertesta* with full certainty as a part of the carapace and not cervical or caudal osteoderms (especially keeping in mind that these elements are strictly homologous), there are several aspects that may indicate that they indeed contributed to the carapace. Firstly, the cervical and caudal osteoderms in *Prog. quenstedti* are organized in tetrads (with two large spikes located in between two smaller spikes) and triads (with all spikes more or less the same size, despite minor asymmetries), respectively (Gaffney 1990). The most complete osteoderm of *C. tenertesta*, however, is built from two spikes of clearly differing size, and there is a base of a third spike located lateral to the smaller spike. Given that the spikes are laterally asymmetrical and that the larger element is more likely to be located medially, this would mean that there were at least six spikes in the row. While possible, it is incongruent with morphology observed in *Prog. quenstedti*. Secondly, the spikes are nearly flat on one side and convex on the other. Cervical and caudal osteoderms of *Prog. quenstedti* are round in cross-section, but marginal elements of the carapace frequently show dorsoventral asymmetry. Thirdly, two preserved spikes of *C. tenertesta* are divided by a well-defined sulcus. There is no unambiguous evidence of sulci on cervical or caudal osteoderms of *Prog. quenstedti* (TSz pers. obs. 2014), but sulci are expected to be present between marginal elements of the carapace. Although the affinity between *C. tenertesta* and *Prog. quenstedti* was previously proposed mostly based on the assumption that both taxa share cervical osteoderms (Joyce 2017), even if the discussed specimens are interpreted as marginal parts of the shell, they more closely resemble spiky marginals of *Proganochelys* spp. than the more ovoid posterior marginals of *Proterochersis* spp., still supporting the result of our phylogenetic analysis, with these two genera located along the turtle stem and not forming an exclusive clade (see above). In any case, the complex spikes of *C. tenertesta* are evidence of an osteodermal mosaic in either nuchal or pygal region of the carapace in a Norian turtle other than *Proterochersis* spp. Joyce *et al.* (2009) interpreted one of the carapace fragments (partial costal with exposed rib apex and sutured single peripheral element) as part of the posterior region of the carapace, but the place indicated by them is located behind the pelvis, which makes such a positioning of ribs impossible. We therefore suggest, that this element was located more anteriorly (Fig. 19).

The morphology of the osteodermal mosaic in *Proterochersis* spp., particularly in the posterior part of the carapace, is comparable to the secondary armour of dermochelyids (Gervais 1872; Wood *et al.* 1996), especially of *Dermochelys coriacea* Vandelli, 1761. Peculiarly, early, less derived dermochelyids tended to have a relatively organized layout of osteoderms with rather even edges, while in *D. coriacea* the ossifications are thinner, lack regularity of shape and arrangement, and have serrated sutural edges (Wood *et al.* 1996; Delfino *et al.* 2013; Chen *et al.* 2015) very similar to those of *Proterochersis* spp. The appearance of a pattern of thin, irregular platelets external to the ribs in these two families may suggest some deep, developmental homology of these structures in these two taxa, but the mechanisms of their development are enigmatic even in the latter, and obviously, they are not a direct heritage. Still, there are some prominent differences between the mosaic of *Proterochersis* spp. and *D. coriacea*: the ossicles in the latter are more numerous, proportionally smaller, completely separate from the endoskeleton and cover the whole trunk of the animal. These incongruences may either hint at a different developmental background and complete lack of homology or divergent evolutionary paths despite some common developmental pathways. Possibly future studies will resolve this question.

Supernumerary posterior plastral elements

The homology of the three SPPEs of *Proterochersis* spp. is uncertain. They may potentially be just another row of plastral bones, homologous to gastralia, but we find this interpretation unconvincing due to their position posterior to pelvis and especially given the presence of the medial element (the only other medial plastral element being the entoplastron, a homologue to the interclavicle). Considering the position of these bones at the posterior edge of the ischium and the familiar motif of posterolateral, finger-like processes bracing the cloaca, we

propose their homology with the hypoischium of other Triassic turtles (see below). Alternative, a third possibility is that the SPPEs of *Proterochersis* spp. may represent neomorphic structures nonhomologous to either the hypoischium or gastralia, that substituted for the hypoischium of other Late Triassic pantestudinates.

Our interpretation of the SPPEs as homologues of hypoischium is challenged by four main differences between these elements. Firstly, the hypoischium of the remaining Triassic taxa is located deeper than the plastron, approximately in the same plane as the ventral surface of the ischium (Gaffney 1990; Sterli *et al*. 2007; Li *et al*. 2008) while the SPPEs of *Proterochersis* spp. lie in the same plane as the external surface of the plastron, i.e. their surface is more external than the ventral limit of the ischium. Secondly, the SPPEs in *Proterochersis* spp. were apparently embedded within the osteogenic plastral dermis and bear a plastron-like texture, while the hypoischia of the remaining pantestudinates are smooth and apparently had no intimate contact with the external layers of dermis. Thirdly, the hypoischium of other taxa only articulates with the ischium, while in *Proterochersis* spp. the SPPEs are sutured both to the ischium and to the xiphiplastra. Fourthly, in *Proterochersis* spp. they are covered by a set of three scutes (two caudals and one intercaudal) while there is no trace of any scutes covering the hypoischium in other taxa. The sutures delineating the ischium are unfortunately fully ankylosed in all specimens of *Proterochersis* spp., so it is uncertain whether the whole SPPEs in *Proterochersis* spp. are shifted towards the epidermis in relation to the typical position of hypoischium (in this case, to uphold our proposed homology, the hypoischium would have to migrate several millimetres externally) or if their visceral parts are located completely posterior to the ischium as the hypoischium of other pantestudinates, and only have a surplus layer of dermal bone, expanding them ventrally (this would require either a minor external migration of the hypoischium or thickening of the osteogenic plastral dermis to engulf the ventral parts of the hypoischium, the latter possibly also facilitating the strong osseous connection present between the proterochersid plastron and pelvis). In both cases, our hypothesis would require these elements to develop a sutural contact with the xiphiplastra, which in proterochersids lie in the same plane as the posterior plastral bones and reach more posteriorly than in other pantestudinates, covering the pelvis ventrally (Gaffney 1990; Sterli *et al*. 2007; Li *et al*. 2008; Szczygielski & Sulej 2016). It is impossible to ascertain whether the caudal and intercaudal scutes were present in other pantestudinates (if so, they could leave no sulci on the hypoischium because it was located deeper than the plastral bones and separated from the scutes by a thicker layer of tissue), or if these scutes are an autapomorphy of Proterochersidae or *Proterochersis* spp. These mentioned differences seem to be correlated with each other and stem from the embedding of the supposed hypoischium (SPPEs) within the plastral dermis. We speculate that the changes in that region could be akin to the processes occurring during the evolution of other plastral bones from the clavicles, interclavicle and gastralia, and carapace elements from ribs, cleithra and neural processes. If our hypothesis is correct, the presence of a hypoischium in proterochersids refutes the homology of their anal notch with that of pleurodires, further strengthening their position as early stem turtles. Unfortunately, the posteriormost part of the plastron is destroyed in *Keuperotesta limendorsa*, so it is unknown whether the SPPEs are diagnostic for Proterochersidae as a whole or only for the genus *Proterochersis*. Joyce *et al*. (2013) reported the presence of the hypoischium in *Keuperotesta limendorsa* holotype (SMNS 17757, at the time identified as *Proterochersis robusta*) but the bony element they indicated is in fact the posterior process of the ischia.

The shortening of the hypoischium in comparison to other pantestudinates may partially result from development of the central plastral concavity, similar to that of some modern male turtles (Pritchard 2008; Leuteritz & Gantz 2013), which helps with proper alignment during copulation. The plastron of *Palaeochersis talampayensis*, however, is also concave ventrally (TSu pers. obs. 2016) and this turtle has proportionally the longest hypoischium of all the Triassic turtles (Sterli *et al*. 2007). The geometry of the carapace may therefore also have played a role; both *Proganochelys quenstedti* and *Palaeochersis talampayensis* had flatter shells (Sterli *et al*. 2007 noted that PULR 68 lacks the central part of the carapace making it difficult to evaluate the height of the shell; taking into account the angle at which the remaining parts of the carapace converge dorsally, however, the shell could not possibly be much higher, although some degree of post-mortem compression is also possible; see Szczygielski & Sulej 2018*a*, fig. S3B, D) with low curvature of the posterior rim, low caudal notch and marginal elements protruding posteriorly. *O. semitestacea* probably also lacked an arched back. On the other hand, the shells of *Proterochersis* spp. are higher (even in the apparently flatter *Prot. porebensis*), have steeper posterior region, a higher caudal notch, and their marginalia are directed more ventrally (Szczygielski & Sulej 2018*a*, fig. S3A, C). Thus, the mounting male would be positioned more vertically and closer to the female's cloaca, possibly reducing the need for an elongated hypoischium. The position of cloaca between the caudal processes is supported by the fact that each of SPPEs was covered by an individual scute instead of the posterior expansion of anal scutes. However, more fossils are required to unambiguously ascertain the exact nature and homologies of SPPEs, preferably either

providing an intermediate morphology linking the SPPE to an unmodified hypoischium (thus supporting our hypothesis) or proving the presence of both an SPPE and a hypoischium (thus refuting the homology of these elements).

CONCLUSIONS

During the late nineteenth, nearly all of the twentieth, and even the early twenty-first century there was debate among researchers about whether a dermochelyid-like superficial (epithecal) osteodermal mosaic was plesiomorphic for turtles and subsequently lost or fused with underlying bones (Owen 1849; Baur 1887*a*; Hay 1898, 1922, 1929; Gadow 1909; Versluys 1914*a*, *b*; Deraniyagala 1930; Kälin 1945; Gregory 1946; Lee 1993, 1996, 1997; Scheyer *et al*. 2008; Joyce *et al*. 2009; Lichtig & Lucas 2016) or whether it was a late, dermochelyid-only adaptation (e.g. Zangerl 1939; Cherepanov 1997; and most later authors). The observations presented herein bring a surprising twist to this dispute: the osteodermal mosaic was indeed present in some of the earliest turtles, but it developed after the acquisition of plastron, costal, and neural bones rather than being inherited from some common ancestors of turtles and their non-pantestudinate sister group. In *Proterochersis* spp. it filled the available area between the costals and carapacial rim, and was partially located external to the costals, facilitating the consolidation of the shell. In more derived turtles, the anteriormost and posteriormost costals occupy much of the place covered in *Proterochersis* spp. by the dermal elements, the number of completely dermal elements is much smaller, and their layout is organized, possibly due to interactions with complex, ordered scute pattern. This scenario generally agrees with hypothesis of Cherepanov (1997), although he considered the substitution of overlying osteoderms by underlying costals unlikely due to functional reasons and possibly developmental complications. We argue that evolutionary fixation of a lower number of ossifications (and thus, the connections between them) in the shell was functionally beneficial, because it increased its stiffness and resistance to crushing and bending (Jaslow 1990; Achrai *et al*. 2014), which were primary sources of damage caused by large predators. The developmental complications might have been easily solved by heterochronic changes to the time of ossification of particular shell elements and by optimization of costal development, which would allow them to establish contact with superficial layers of dermis earlier and shield larger area of the dorsum. Development of varied internal morphologies of sutures early in shell evolution indicates optimization towards various stresses and proves that the protective characteristics of the shell were an important factor in the Late Triassic.

Our observations also prove that the armour of tetrapods does not necessarily have to result from a single developmental programme, but may be an effect of numerous interplaying pathways that supplement each other and may even in some ways compete and supersede one another under adaptive selection (e.g. the endoskeleton-derived costal bones crowd out the overlying mosaic of dermal osteoderms). Finally, they stress the need for an in-depth study of the developmental factors responsible for the positioning and formation of osteoderms.

AUTHOR CONTRIBUTIONS

TSz participated in excavations, prepared most of the *Proterochersis porebensis* material, first-hand studied and photographed the material of *Prot. porebensis*, *Prot. robusta*, *Keuperotesta limendorsa*, *Proganochelys quenstedti*, *Pappochelys rosinae*, and *Priscochelys hegnabrunnensis*, analysed and interpreted the data, wrote the manuscript, and prepared the figures and the supplement. TSu participated in excavations, prepared part of the *Proterochersis porebensis* material, first-hand studied and photographed the material of *Odontochelys semitestacea*, *Palaeochersis talampayensis*, and *Chinlechelys tenertesta*, helped with interpretations, and reviewed the manuscript.

Acknowledgements. We thank Rainer Schoch for granting access to the SMNS collection and the loan of SMNS 17755a, Gabriela A. Cisterna for granting access to the PULR collection, Spencer Lucas for granting access to the NMMNH collection, Jun Liu for granting access to IVPP collection, Carl Schweizer for granting access to CSMM collection, Łucja Fostowicz-Frelik and Justyna Słowiak for macrophotographs of *Prot. porebensis* and *Prot. robusta* and histological consultation, Dawid Dróżdż for preparation of the 3D model of ZPAL V.39/22, Marian Dziewiński for additional photographs of ZPAL V.39/20, Krzysztof Karczewski and Szymon Łukasiewicz (Military University of Technology, Warsaw) for production of the CT-scans of SMNS 17755a and ZPAL V.39/22, Robert Bronowicz for histological sections of ZPAL V.39/20, Piotr Bajdek for additional preparation work, as well as the Editor, Juliana Sterli, an anonymous reviewer, and the Production Office for their valuable suggestions and work needed to process and improve this manuscript. TSz is supported by the National Science Centre (Narodowe Centrum Nauki), Poland, grant no. 2016/23/N/NZ8/01823. TSu was supported during the early stages of this study by the National Science Centre (Narodowe Centrum Nauki), Poland, grant no. 2012/07/B/NZ8/02707.

DATA ARCHIVING STATEMENT

Data for this study are available in the Dryad Digital Repository: https://doi.org/10.5061/dryad.b23d7k8

Editor. Roger Benson

REFERENCES

ACHRAI, B., BAR-ON, B. and WAGNER, H. D. 2014. Bending mechanics of the red-eared slider turtle carapace. *Journal of the Mechanical Behavior of Biomedical Materials*, **30**, 223–233.

ANQUETIN, J. and JOYCE, W. G. 2014. A reassessment of the Late Jurassic turtle *Eurysternum wagleri* (Eucryptodira, Eurysternidae). *Journal of Vertebrate Paleontology*, **34**, 1317–1328.

—— BARRETT, P. M., JONES, M. E. H., MOORE-FAY, S. and EVANS, S. E. 2009. A new stem turtle from the Middle Jurassic of Scotland: new insights into the evolution and palaeoecology of basal turtles. *Proceedings of the Royal Society B*, **276**, 879–886.

—— PÜNTENER, C., BILLON-BRUYAT, J.-P., SCHNEIDER, R., PÜNTENER, C. and BILLON-BRUYAT, J.-P. 2014. A taxonomic review of the Late Jurassic eucryptodiran turtles from the Jura Mountains (Switzerland and France). *PeerJ*, **2**, e369.

BAUR, G. 1887*a*. On the morphogeny of the carapace in Testudinata. *The American Naturalist*, **21**, 89–90.

—— 1887*b*. Ueber den Ursprung der Extremitäten der Ichthyopterygia. *Berichte Über Versammlungen des Oberrheinischen Vereines*, **20**, 17–20.

BROIN, F. DE 1984. *Proganochelys ruchae* n.sp., chélonien du Trias supérieur de Thaïlande. *Studia Palaeocheloniologica*, **1**, 87–97.

—— INGAVAT, R., JANVIER, P. and SATTAYARAK, N. 1982. Triassic turtle remains from northeastern Thailand. *Journal of Vertebrate Paleontology*, **2**, 41–46.

BURKE, A. C. 1989. Development of the turtle carapace: implications for the evolution of a novel bauplan. *Journal of Morphology*, **199**, 363–378.

—— 1991. The development and evolution of the turtle body plan: inferring intrinsic aspects of the evolutionary process from experimental embryology. *American Zoologist*, **31**, 616–627.

CEBRA-THOMAS, J. A., TAN, F., SISTLA, S., ESTES, E., BENDER, G., KIM, C., RICCIO, P. and GILBERT, S. F. 2005. How the turtle forms its shell: a paracrine hypothesis of carapace formation. *Journal of Experimental Zoology B: Molecular & Developmental Evolution*, **304**, 558–569.

CHEN, I. H., YANG, W. and MEYERS, M. A. 2015. Leatherback sea turtle shell: a tough and flexible biological design. *Acta Biomaterialia*, **28**, 2–12.

CHEREPANOV, G. O. 1989. New morphogenetic data on the turtle shell: discusion on the origin of the horny and bony parts. *Studia Geologica Salmanticensia*, **3**, 9–24.

—— 1997. The origin of the bony shell of turtles as a unique evolutionary model in reptiles. *Russian Journal of Herpetology*, **4**, 155–162.

—— 2016. Nature of the turtle shell: morphogenetic causes of bone variability and its evolutionary implication. *Paleontological Journal*, **50**, 1641–1648.

CIGNONI, P., CALLIERI, M., CORSINI, M., DELLEPIANE, M., GANOVELLI, F. and RANZUGLIA, G. 2008. MeshLab: an open-source mesh processing tool. 129–136. *In 6th Eurographics Italian Chapter Conference*. Eurographics Association.

DELFINO, M., SCHEYER, T. M., CHESI, F., FLETCHER, T., GEMEL, R., MACDONALD, S., RABI, M. and SALISBURY, S. W. 2013. Gross morphology and microstructure of type locality ossicles of *Psephophorus polygonus* Meyer, 1847 (Testudines, Dermochelyidae). *Geological Magazine*, **150**, 767–782.

DERANIYAGALA, P. E. P. 1930. Testudinate evolution. *Proceedings of the Zoological Society of London*, **100**, 1057–1070.

FRAAS, E. 1913. *Proterochersis*, eine pleurodire Schildkröte aus dem Keuper. *Jahreshefte des Vereins für Vaterlandische Naturkunde in Württemberg*, **69**, 13–30.

GADOW, H. 1909. *Amphibia and reptiles*. MacMillan & Co., London.

GAFFNEY, E. S. 1985. The shell morphology of the Triassic turtle *Proganochelys*. *Neues Jahrbuch für Geologie und Paläontologie, Abhandlungen*, **170**, 1–26.

—— 1990. The comparative osteology of the Triassic turtle *Proganochelys*. *Bulletin of the American Museum of Natural History*, **194**, 1–263.

GERVAIS, P. 1872. Ostéologie du sphargis luth (*Sphargis coriacea*). *Nouvelles Archives du Muséum d'Histoire naturelle de Paris*, **8**, 234.

GILBERT, S. F., LOREDO, G. A., BRUKMAN, A. and BURKE, A. C. 2001. Morphogenesis of the turtle shell: the development of a novel structure in tetrapod evolution. *Evolution & Development*, **3**, 47–58.

—— CEBRA-THOMAS, J. A. and BURKE, A. C. 2008. How the turtle gets its shell. 1–16. *In* WYNEKEN, J., GODFREY, M. H. and BELS, V. (eds). *Biology of turtles*. CRC Press.

GOLOBOFF, P. A., FARRIS, J. S. and NIXON, K. C. 2008. TNT, a free program for phylogenetic analysis. *Cladistics*, **24**, 774–786.

GREGORY, W. K. 1946. Pareiasaurs versus placodonts as near ancestors to the turtles. *Bulletin of the American Museum of Natural History*, **86**, 279–326.

HAY, O. P. 1898. On *Protostega*, the systematic position of *Dermochelys*, and the morphogeny of the chelonian carapace and plastron. *The American Naturalist*, **32**, 929–948.

—— 1922. On the phylogeny of the shell of the Testudinata and the relationships of *Dermochelys*. *Journal of Morphology*, **36**, 421–445.

—— 1929. Further consideration of the shell of *Chelys* and of the constitution of the armor of turtles in general. *Proceedings of the United States National Museum*, **73**, 1–12.

HORNUNG, J. and AIGNER, T. 1999. Reservoir and aquifer characterization of fluvial architectural elements: Stubensandstein, Upper Triassic, southwest Germany. *Sedimentary Geology*, **129**, 215–280.

JASLOW, C. R. 1990. Mechanical properties of cranial sutures. *Journal of Biomechanics*, **23**, 313–321.

JENKINS, F. A., SHUBIN, N. H., AMARAL, W. W., GATESY, S. M., SCHAFF, C. R., CLEMMENSEN, L. B., DOWNS, W. R., DAVIDSON, A. R., BONDE, N. and OSBAECK, F. 1994. Late Triassic continental vertebrates and depositional environments of the Fleming Fjord Formation, Jameson Land, East Greenland. *Meddelelser om Grønland, Geoscience*, **32**, 1–25.

JOYCE, W. G. 2000. The first complete skeleton of *Solnhofia parsonsi* (Cryptodira, Eurysternidae) from the Upper Jurassic of Germany and its taxonomic implications. *Journal of Paleontology*, **74**, 684–700.

—— 2017. A review of the fossil record of basal Mesozoic turtles. *Bulletin of the Peabody Museum of Natural History*, **58**, 65–113.

—— and KARL, H.-V. 2006. The world's oldest fossil turtle: fact versus fiction. *Fossil Turtle Research*, **1**, 104–111.

—— LUCAS, S. G., SCHEYER, T. M., HECKERT, A. B. and HUNT, A. P. 2009. A thin-shelled reptile from the Late Triassic of North America and the origin of the turtle shell. *Proceedings of the Royal Society B*, **276**, 507–513.

—— SCHOCH, R. R. and LYSON, T. R. 2013. The girdles of the oldest fossil turtle, *Proterochersis robusta*, and the age of the turtle crown. *BMC Evolutionary Biology*, **13**, 266.

—— RABI, M., CLARK, J. M. and XU, X. 2016. A toothed turtle from the Late Jurassic of China and the global biogeographic history of turtles. *BMC Evolutionary Biology*, **16**, 236.

KÄLIN, J. 1945. Zur Morphogenese des Panzers bei den Schildkröten. *Acta Anatomica*, **1**, 144–176.

KARL, H.-V. 2005. The homology of supramarginals in turtles (Reptilia: Chelonii). *Studia Geologica Salmanticensia*, **41**, 63–75.

KORDIKOVA, E. G. 2002. Heterochrony in the evolution of the shell of Chelonia. Part 1: Terminology, Cheloniidae, Dermochelyidae, Trionychidae, Cyclanorbidae and Carettochelyidae. *Neues Jahrbuch für Geologie und Paläontologie, Abhandlungen*, **226**, 343–417.

KURATANI, S., KURAKU, S. and NAGASHIMA, H. 2011. Evolutionary developmental perspective for the origin of turtles: the folding theory for the shell based on the developmental nature of the carapacial ridge. *Evolution & Development*, **13**, 1–14.

ICZN 1999. *International Code of Zoological Nomenclature*. 4th edn. International Trust for Zoological Nomenclature. http://www.iczn.org/iczn/index.jsp#

LEE, M. S. Y. 1993. The origin of the turtle body plan: bridging a famous morphological gap. *Science*, **261**, 1716–1720.

—— 1996. Correlated progression and the origin of turtles. *Nature*, **379**, 812–815.

—— 1997. Pareiasaur phylogeny and the origin of turtles. *Zoological Journal of the Linnean Society*, **120**, 197–280.

LEUTERITZ, T. E. J. and GANTZ, D. T. 2013. Sexual dimorphism in radiated tortoises (*Astrochelys radiata*). *Chelonian Research Monographs*, **6**, 105–112.

LI, C., WU, X.-C., RIEPPEL, O. C., WANG, L.-T. and ZHAO, L.-J. 2008. An ancestral turtle from the Late Triassic of southwestern China. *Nature*, **456**, 497–501.

LICHTIG, A. J. and LUCAS, S. G. 2015. New insights into the ecology and ancestry of Triassic turtles. 40–41. *In 13th Annual Symposium on the Conservation and Biology of Tortoises and Freshwater Turtles. Program & Abstracts*.

—— —— 2016. *Chinlechelys*: A reexamination of North America's oldest (Triassic, Revueltian, Norian) turtle and its impact on theories of turtle origins. 175. *In* FARKE, A., MACKENZIE, A. and MILLER-CAMP, J. (eds). *Society of Vertebrate Paleontology, 76th Annual Meeting Program & Abstracts*.

LIMAYE, A. 2012. Drishti, a volume exploration and presentation tool. *Proceedings of SPIE*, **8506**, 85060X.

LOREDO, G. A., BRUKMAN, A., HARRIS, M. P., KAGLE, D., LECLAIR, E. E., GUTMAN, R., DENNEY, E., HENKELMAN, E., MURRAY, B. P., FALLON, J. F., TUAN, R. S. and GILBERT, S. F. 2001. Development of an evolutionarily novel structure: fibroblast growth factor expression in the carapacial ridge of turtle embryos. *Journal of Experimental Zoology*, **291**, 274–281.

LUCAS, S. G., HECKERT, A. B. and HUNT, A. P. 2000. Probable turtle from the Upper Triassic of east-central New Mexico. *Neues Jahrbuch für Geologie und Paläontologie – Monatshefte*, **5**, 287–300.

LYSON, T. R., SCHACHNER, E. R., BOTHA-BRINK, J., SCHEYER, T. M., LAMBERTZ, M., BEVER, G. S., RUBIDGE, B. S. and DE QUEIROZ, K. 2014. Origin of the unique ventilatory apparatus of turtles. *Nature Communications*, **5**, 5211.

MAUTNER, A.-K., LATIMER, A. E., FRITZ, U. and SCHEYER, T. M. 2017. An updated description of the osteology of the pancake tortoise *Malacochersus tornieri* (Testudines: Testudinidae) with special focus on intraspecific variation. *Journal of Morphology*, **278**, 321–333.

McEWAN, B. 1982. Bone anomalies in the shell of *Gopherus polyphemus*. *Florida Scientist*, **45**, 189–195.

MOUSTAKAS-VERHO, J. E., CEBRA-THOMAS, J. and GILBERT, S. F. 2017. Patterning of the turtle shell. *Current Opinion in Genetics & Development*, **45**, 124–131.

NAGASHIMA, H., KURAKU, S., UCHIDA, K., OHYA, Y. K., NARITA, Y. and KURATANI, S. 2007. On the carapacial ridge in turtle embryos: its developmental origin, function and the chelonian body plan. *Development*, **134**, 2219–2226.

—— SUGAHARA, F., TAKECHI, M., ERICSSON, R., OHYA, Y. K., NARITA, Y. and KURATANI, S. 2009. Evolution of the turtle body plan by the folding and creation of new muscle connections. *Science*, **325**, 193–196.

—— KURAKU, S., UCHIDA, K., OHYA, Y. K., NARITA, Y. and KURATANI, S. 2012. Body plan of turtles: an anatomical, developmental and evolutionary perspective. *Anatomical Science International*, **87**, 1–13.

—— —— —— —— —— —— 2013*a*. Origin of the turtle body plan: the folding theory to illustrate turtle-specific developmental repatterning. 37–50. *In* BRINKMAN D. B., HOLROYD, P. A. and GARDNER, J. D. (eds). *Morphology and evolution of turtles*. Springer Science+Business Media.

—— HIRASAWA, T., SUGAHARA, F., TAKECHI, M., USUDA, R., SATO, N. and KURATANI, S. 2013*b*. Origin of the unique morphology of the shoulder girdle in turtles. *Journal of Anatomy*, **223**, 547–556.

NIEDŹWIEDZKI, G., BRUSATTE, S. L., SULEJ, T. and BUTLER, R. J. 2014. Basal dinosauriform and theropod dinosaurs from the mid-late Norian (Late Triassic) of Poland: implications for Triassic dinosaur evolution and distribution. *Palaeontology*, **57**, 1121–1142.

NOPCSA, F. B. 1923. *Die Familien der Reptilien*. Gebrüder Borntraeger, Berlin.

OWEN, R. 1849. On the development and homologies of the carapace and plastron of the chelonian reptiles. *Philosophical Transactions of the Royal Society of London*, **139**, 151–171.

—— 1876. *Descriptive and illustrated catalogue of the fossil Reptilia of South Africa in the collection of the British Museum*. Taylor & Francis, London.

PARKER, W. G. 2018. Redescription of *Calyptosuchus* (*Stagonolepis*) *wellesi* (Archosauria: Pseudosuchia: Aetosauria) from the Late Triassic of the Southwestern United States with a discussion of genera in vertebrate paleontology. *PeerJ*, **6**, e4291.

PÉREZ-GARCÍA, A. and CODREA, V. 2018. New insights on the anatomy and systematics of *Kallokibotion* Nopcsa, 1923, the enigmatic uppermost Cretaceous basal turtle (stem Testudines) from Transylvania. *Zoological Journal of the Linnean Society*, **182**, 419–443.

PRITCHARD, P. C. H. 2008. Evolution and structure of the turtle shell. 46–83. *In* WYNEKEN, J., GODFREY, M. H. and BELS, V. (eds). *Biology of turtles*. CRC Press.

RICE, R., RICCIO, P., GILBERT, S. F. and CEBRA-THOMAS, J. A. 2015. Emerging from the rib: resolving the turtle controversies. *Journal of Experimental Zoology B: Molecular & Developmental Evolution*, **324**, 208–220.

—— KALLONEN, A., CEBRA-THOMAS, J. A. and GILBERT, S. F. 2016. Development of the turtle plastron, the order-defining skeletal structure. *Proceedings of the National Academy of Sciences*, **113**, 5317–5322.

RIEPPEL, O. C. 2002. The dermal armor of the cyamodontoid placodonts (Reptilia, Sauropterygia): morphology and systematic value. *Fieldiana Geology*, **46**, 1–41.

ROUGIER, G. W., DE LA FUENTE, M. S. and ARCUCCI, A. B. 1995. Late Triassic turtles from South America. *Science*, **268**, 855–858.

SCHEYER, T. M. 2008. Aging the oldest turtles: the placodont affinities of *Priscochelys hegnabrunnensis*. *Naturwissenschaften*, **95**, 803–810.

—— and DESOJO, J. B. 2011. Palaeohistology and external microanatomy of rauisuchian osteoderms (Archosauria: Pseudosuchia). *Palaeontology*, **54**, 1289–1302.

—— and SANDER, P. M. 2007. Shell bone histology indicates terrestrial palaeoecology of basal turtles. *Proceedings of the Royal Society B*, **247**, 1885–1893.

—— BRÜLLMANN, B. and SÁNCHEZ-VILLAGRA, M. R. 2008. The ontogeny of the shell in side-necked turtles, with emphasis on the homologies of costal and neural bones. *Journal of Morphology*, **269**, 1008–1021.

—— DESOJO, J. B. and CERDA, I. A. 2014. Bone histology of phytosaur, aetosaur, and other archosauriform osteoderms (Eureptilia, Archosauromorpha). *Anatomical Record*, **297**, 240–260.

SCHINDELIN, J., ARGANDA-CARRERAS, I., FRISE, E., KAYNIG, V., LONGAIR, M., PIETZSCH, T., PREIBISCH, S., RUEDEN, C., SAALFELD, S., SCHMID, B., TINEVEZ, J.-Y., WHITE, D. J., HARTENSTEIN, V., ELICEIRI, K., TOMANCAK, P. and CARDONA, A. 2012. Fiji: an open-source platform for biological-image analysis. *Nature Methods*, **9**, 676–682.

SCHOCH, R. R. and SUES, H.-D. 2015. A Middle Triassic stem-turtle and the evolution of the turtle body plan. *Nature*, **523**, 584–587.

—— —— 2016. The diapsid origin of turtles. *Zoology*, **119**, 159–161.

—— —— 2018. Osteology of the Middle Triassic stem-turtle *Pappochelys rosinae* and the early evolution of the turtle skeleton. *Journal of Systematic Palaeontology*, **16**, 927–965.

STERLI, J., DE LA FUENTE, M. S. and ROUGIER, G. W. 2007. Anatomy and relationships of *Palaeochersis talampayensis*, a Late Triassic turtle from Argentina. *Palaeontographica Abteilung A*, **281**, 1–61.

SULEJ, T., NIEDŹWIEDZKI, G. and BRONOWICZ, R. 2012. A new Late Triassic vertebrate fauna from Poland with turtles, aetosaurs, and coelophysoid dinosaurs. *Journal of Vertebrate Paleontology*, **32**, 1033–1041.

SZCZYGIELSKI, T. 2017. Homeotic shift at the dawn of the turtle evolution. *Royal Society Open Science*, **4**, 160933.

—— and SŁOWIAK, J. 2018. Shell variability and sexual dimorphism in the earliest turtles. 79–80. *In 6th Turtle Evolution Symposium. Program & Abstracts*. Scidinge Hall, Tübingen.

—— and SULEJ, T. 2016. Revision of the Triassic European turtles *Proterochersis* and *Murrhardtia* (Reptilia, Testudinata, Proterochersidae), with the description of new taxa from Poland and Germany. *Zoological Journal of the Linnean Society*, **177**, 395–427.

—— —— 2018*a*. Data from: The early composition and evolution of the turtle shell (Reptilia, Testudinata). *Dryad Digital Repository*. https://doi.org/10.5061/dryad.b23d7k8

—— —— 2018*b*. Osteodermal mosaic in the carapace of the earliest turtles. 2–5. *In 6th Turtle Evolution Symposium. Program & Abstracts*. Scidinge Hall, Tübingen.

SZULC, J., RACKI, G., JEWUŁA, K. and ŚRODOŃ, J. 2015. How many Upper Triassic bone-bearing levels are there in Upper Silesia (Southern Poland)? A critical overview of stratigraphy and facies. *Annales Societatis Geologorum Poloniae*, **85**, 587–626.

VALLÉN, E. 1942. Beiträge zur Kenntnis der Ontogenie und der vergleichenden Anatomie des Schildkrötenpanzers. *Acta Zoologica*, **23**, 1–127.

VANDELLI, D. 1761. *Epistola de holothurio, et testudine coriacea ad celebrrimum Carolum Linnaeum*. Conzatti, Padova.

VERSLUYS, J. 1914*a*. On the phylogeny of the carapace, and on the affinities of the leathery turtle, *Dermochelys coriacea*. *Report of the British Association for the Advancement of Science*, **38**, 791–807.

—— 1914*b*. Über die Phylogenie des Panzers der Schildkröten und über die Verwandtschaft der Lederschildkröte (*Dermochelys coriacea*). *Zeitschrift für Palaeontologie*, **1**, 321–347.

WALKER, W. F. 1947. The development of the shoulder region of the turtle, *Chrysemys picta marginata*, with special reference to the primary musculature. *Journal of Morphology*, **80**, 195–249.

WESTPHAL, F. 1975. Bauprinzipien im Panzer der Placodonten (Reptilia triadica). *Paläontologische Zeitschrift*, **49**, 97–125.

WOOD, R. C., JOHNSON-GROVE, J., GAFFNEY, E. S. and MALEY, K. F. 1996. Evolution and phylogeny of leatherback turtles (Dermochelyidae), with descriptions of new fossil taxa. *Chelonian Conservation & Biology*, **2**, 266–286.

ZANGERL, R. 1939. The homology of the shell elements in turtles. *Journal of Morphology*, **65**, 383–409.

—— 1969. The turtle shell. 311–339. *In* GANS, C. (ed.) *Biology of the Reptilia. Vol. 1*. Academic Press.

—— and JOHNSON, R. G. 1957. The nature of shield abnormalities in the turtle shell. *Fieldiana Geology*, **10**, 341–362.

ZATOŃ, M., NIEDŹWIEDZKI, G., MARYNOWSKI, L., BENZERARA, K., POTT, C., COSMIDIS, J., KRZYKAWSKI, T. and FILIPIAK, P. 2015. Coprolites of Late Triassic carnivorous vertebrates from Poland: an integrative approach. *Palaeogeography, Palaeoclimatology, Palaeoecology*, **430**, 21–46.